NISTIR 6233

Preliminary Investigations Into Corrosion in Anti-Lock Braking Systems

R. E. Ricker, J. L. Fink, A. J. Shapiro, L. C. Smith, and R. J. Schaefer

Metallurgy Division

Materials Science and Engineering Laboratory
National Institute of Standards and Technology
Technology Administration
U.S. Department of Commerce

Gaithersburg, MD 20899

September 24, 1998

Final Report
Interagency Agreement No. DTNH22-97-X-01250

Prepared for:

National Highway Traffic Safety Administration
U.S. Department of Transportation

United States Department of Commerce
National Institute of Standards and Technology

NISTIR 6233

Preliminary Investigations Into Corrosion in Anti-Lock Braking Systems

R. E. Ricker
J. L. Fink
A. J. Shapiro
L. C. Smith
R. J. Schaefer

U.S. DEPARTMENT OF COMMERCE
Technology Administration
National Institute of Standards and Technology
Metallurgy Division
Materials Science and Engineering Laboratory
Gaithersburg, MD 20899

Prepared for:
National Highway Traffic Safety Administration
U.S. Department of Transportation

September 24, 1998

U.S. DEPARTMENT OF COMMERCE
William M. Daley, Secretary

TECHNOLOGY ADMINISTRATION
Gary R. Bachula, Acting Under Secretary for Technology

NATIONAL INSTITUTE OF STANDARDS
AND TECHNOLOGY
Raymond G. Kammer, Director

PRELIMINARY INVESTIGATIONS INTO CORROSION IN ANTI-LOCK BRAKING SYSTEMS

R. E. Ricker, J. L. Fink, A. J. Shapiro,
L. C. Smith, and R. J. Schaefer

Metallurgy Division
Materials Science and Engineering Laboratory
National Institute of Standards and Technology
Technology Administration, US Dept. of Commerce
Gaithersburg, MD 20899

1.0 INTRODUCTION

Preliminary studies into the nature and scope of metallic corrosion in motor vehicle brake fluids were conducted at NIST at the request of the National Highway Transportation Safety Administration (NHTSA). The focus of this study is on developing an understanding of how the corrosivity of brake fluids may change as they age in service, developing an understanding of the mechanism of this change, and conducting some preliminary experiments to evaluate the difficulty of developing a laboratory measurement technique for quantifying these changes. The influence of corrosion on the function or performance of any type of braking system or evaluation of the performance of types of brake fluids[1] is outside the scope of this research and, therefore, is not addressed.

2.0 BACKGROUND

2.1 Motor Vehicle Brake Fluid Standards

In the United States, for a hydraulic fluid to qualify for use as a brake fluid in motor vehicles it must pass the requirements of Standard Number 116 of the Federal Motor Vehicle Safety Standards section of the National Highway Traffic Safety Administration Chapter of the Code of Federal Regulations (49 CFR 571.116) [1]. This standard is a performance standard which does not specify any particular brake fluid chemistry or range of compositions, but it does specify 14 different types of experiments and measurements with three different performance levels for brake fluids identified as DOT 3, DOT 4, and DOT 5. The primary difference between these three brake fluids is in their physical properties such as boiling points (wet and dry) and viscosities. All three brake fluids must meet the same corrosion and elastomer compatibility requirements. SAE International also has a brake fluid standard (J1703), but the corrosion test in this standard is essentially identical to the Federal standard (49 CFR 571.116) [2]. Since DOT 3 brake fluids qualify for use in passenger vehicles and light trucks, they represent the vast majority of brake fluid environments in ABS equipped vehicles and this work focusses on DOT 3 brake fluids.

[1]Certain trade names and company products may be mentioned in the text, tables, or illustrations in order to specify adequately the experiments conducted. In no case does such identification imply recommendation or endorsement by the National Institute of Standards and Technology, nor does it imply that the products are neccessarily the best available for the purpose.

The corrosion tests in these standards consist of placing an array of 6 polished, cleaned, and weighed strips 80 mm long and 13 mm wide of copper, brass, cast iron, aluminum, steel, and tinned iron into a mixture of 380 mL of the subject brake fluid with 20 mL of distilled water added. Then, the jar containing the solution, the samples, and a standard wheel cylinder cup is sealed and placed into an oven at 100 °C. After 120 hours, the samples are cooled, cleaned, examined, dried, and weighed. From these measurements, the weight change per unit area is determined for each of the samples. The maximum allowable mass change per unit surface area for each alloy in this standard is given in Table I. This table also includes corrosion data published by Jackson et al.[3] for corrosion weight changes for a brake fluid base with no additives in this experiment. From this table, it can be seen that a brake fluid made from good quality materials can pass this standard without the addition of any corrosion inhibitors.

2.2 Brake Fluid Chemistry

In the 1920's, when automobiles started switching to hydraulic brakes, the only material available for the required flexible hoses was natural rubber. As a result, a hydraulic fluid compatible with natural rubber was required for this application and a mixture of castor oil and alcohol was found to meet this need. The use of this fluid enabled the development of hydraulic brakes in the 1920's before synthetic rubbers became available. However, it fixed this industry on the use of hydraulic fluids based on glycols, glycol ethers, alcohols, polyglycols and other related compounds that can be used with elastomeric braking system components made of natural rubber, styrene, butadiene, ethylene, propylene rubber, or polychloroprene. As a result, brake fluids are completely different from any of the other fluids used in automotive systems [4].

As mentioned above, the standard for DOT 3 brake fluid (49 CFR 571.116) is a performance standard which does not specify any particular brake fluid chemistry or range of compositions, but it includes elastomer compatibility, boiling point, and other requirements that limit the range of chemical compounds that industry can select from in developing their brake fluid formulation [1]. Since industry is free to develop and market any fluid that meets the performance requirements of this standard, companies have developed proprietary compositions and a wide variety of mixtures are commercially available. To obtain an idea of the range of compositions present in commercial brake fluids, Materials Safety and Data Sheets (MSDS's) from 6 different brake fluid suppliers were examined and Table II is a compilation of the compounds as identified in these MSDS's. As pointed out by Rabold [5], these complex mixtures are easier to understand if the compounds are grouped into four categories based on their function in the brake fluid formulation:

(1) Solvent Base (diluent) - Glycol ethers or mixtures of glycol ethers are typically used for the bulk of a brake fluid because they have high boiling points at relatively low molecular weights (low viscosities). These compounds are primarily responsible for the properties such as boiling point, viscosity, and elastomer compatibility. There are over a dozen different types of glycol ethers used in brake fluids each with slightly different properties. Different manufacturers may select different compounds or proportions for their formulations.

(2) Solvent modifiers - Glycols are commonly added to improve the properties of the solvent. Typically they are used to increase the solubility of additives or to improve elastomer compatibility. As with glycol ethers, there are a number of different glycols that can be selected for a brake fluid formulation.

(3) Lubricants - Polyglycols are commonly added to brake fluid formulations to improve

lubrication. These are simply higher molecular weight versions of the glycols and a wide range of molecular weights and compositions are possible.

(4) Additives - Corrosion inhibitors, pH stabilizers, and antioxidants are commonly added to brake fluid formulations to improve long term performance of these brake systems and to insure that the formulations pass the corrosion tests in the standards.

2.3 Brake Fluid Chemistry Variations and Aging in Service

Knowledge of the chemistry of the original equipment manufacturer (OEM) brake fluid put into new vehicles is important in understanding the origins of corrosion of the metals exposed to brake fluid in ABS equipped vehicles. However, as vehicles age, the chemistry of their brake fluids will change and will do so at different rates depending on variety of factors. That is, when a fleet of identical vehicles filled with identical brake fluids are put into service, the initial chemistry of the brake fluid environments in these vehicles will fit into a narrow spectrum or range of compositions. However, as these vehicles age and see different service conditions the range of brake fluid chemistries in these vehicles will broaden and understanding the effects of these deviations from the ideal new vehicle chemistry on corrosion could be more important than understanding corrosion in fresh OEM brake fluid.

The factors that contribute to alterations in brake fluid chemistry as a vehicle ages can be grouped into three categories: (1) intrinsic factors, (2) extrinsic factors, and (3) abnormal events. Intrinsic factors are those that depend on the brake fluid chemistry and the design of the ABS system. The chemical and thermal stability of the compounds in the brake fluid are the primary intrinsic factors governing brake fluid degradation during vehicle aging. However, ABS and brake system design factors including the metals and polymers exposed to the brake fluid, the normal temperatures of these materials, the rate of absorption of brake fluid constituents into the polymers, the permeation rate of environmental species through polymers and seals to the brake fluid, and brake fluid circulation rates are also important intrinsic factors. Extrinsic factors are those which depend on the operation of the vehicle, the external environment the vehicle sees in service, vehicle maintenance, and abnormal conditions or events that occur during service. The operator and the driving habits of the operator will determine the mean and the extreme conditions of braking force, wheel cylinder temperatures, and frequency of ABS events. Factors in the external service environment such as temperature, humidity, availability of aggressive chemical species (e.g. NaCl) and road surface conditions (e.g. inclination, rocks, dust , etc.) can all influence the rate of change in brake fluid chemistry. Also, the frequency of maintenance, the choice of maintenance provider, the provider's brake service procedures, and the provider's choice of brake fluid to replace or replenish the brake fluid lost during service will all contribute to the variability of brake fluid environments in vehicles. Finally, abnormal events in the service history of a vehicle can have a dramatic influence on the chemistry of the fluid in that vehicle. Examples of this include collisions with brake fluid loss or an event that influences the integrity of a seal or the permeation rate of environmental species through a hose. This could be as simple as failure to make a secure seal after checking the brake fluid level or as dramatic as a vehicle striking a rock large enough to damage the rotor, caliper, wheel cylinder, brake lines, or hoses. While it is difficult to incorporate all of these factors in a study of brake fluid corrosion, one needs to keep these possibilities in mind when attempting to understand the range of corrosion observed in a fleet of a particular type of vehicle or ABS system. However, the probability that a vehicle's brake fluid will be completely or partially replaced by any readily available aftermarket DOT 3 brake fluid at some time during its service life is so high that it should be incorporated into a corrosion study of this type.

Jackson et al. [3] studied the changes that occur in brake fluid chemistry during vehicular service. They measured the buffering capacity, inhibitor concentrations, and metal ion concentrations in samples of brake fluid removed from vehicles following service for up to 40 months. They found that the buffer capacity and inhibitor concentrations dropped to less than 10% of their initial levels after only 30 months of service. They also found that while the concentrations of copper and zinc ions in the samples increased slowly and continuously from the beginning, that the iron ion content did not begin increasing until after 30 months of service when inhibitor concentrations dropped and dissolved copper levels reached a mass fraction of about 2×10^{-4} (200 ppm). They estimated the rate of copper corrosion from these measurements to be about 25% of the maximum allowed for DOT 3 brake fluid in the Federal Motor Vehicle Safety Standard (49 CFR Part 571.116) [1]. Iron corrosion is not commonly observed in tests conducted with fresh brake fluid and the induction time for iron corrosion observed in this work probably explains the difficulty in reproducing iron corrosion in laboratory experiments. Jackson et al. [3] observed corrosion damage on cast iron components removed from some of these vehicles and found corrosion pits "surrounded by metallic copper." These authors then developed a laboratory aging process for accelerated aging of brake fluids that yielded brake fluid samples with chemistries similar to those observed in the samples removed from the vehicles. They reported that these "laboratory aged" brake fluids could reproduce long term corrosion damage when used in short term vehicular tests. However, they were unable to reproduce worst-case long-term vehicular corrosion damage in laboratory corrosion tests with these "laboratory-aged" brake fluids, but "vehicle-aged" brake fluids also failed to produce this type of damage when used in laboratory corrosion tests [3].

2.4 Metals in ABS Systems

Most ABS equipped brake systems expose a wide range of different metals and alloys to the brake fluid. Aluminum alloy die castings, steels, stainless steels, cast irons, and copper alloys are typically found in ABS systems, master cylinders, brake lines, and wheel cylinders. However, in a typical vehicle the inside surface of the brake lines is the vast majority of the metallic surface area exposed to the brake fluid. A typical light duty vehicle will have approximately 14 m of brake lines and about 0.9 L of brake fluid [3]. Figure 1 is a metallurgical cross section prepared at NIST of a brake line sample supplied by NHTSA. In this figure, it can be seen that these pipes are made from a 2 layer spiral wrap of steel brazed with a copper brazing alloy. Examination of the inside diameter of a brake line at the braze joint, Figure 2, shows that the copper brazing alloy is exposed to the brake fluid and that a significant portion of the inside surface of the brake line is coated with the copper brazing alloy. Jackson et al. [3] estimated that the brake fluid in a typical vehicle is exposed to about 0.12 m^2 of this copper alloy so that copper corrosion rates, well below that required for DOT 3 brake fluids, can result in appreciable copper ion contents in the small volume of brake fluid. In a similar micrograph, Jacobson [6] shows the inside diameter of a brake line after 6 years of service where it appears that all of the copper on the inside surface and for a small distance into the seam has been removed by corrosion.

2.5 Corrosion in ABS Systems

As pointed out by Jackson et al.[3], ABS systems may place greater demands on brake fluids than conventional braking systems. The most significant changes with the addition of ABS to hydraulic brakes are: (1) increased hydraulic pressures, (2) larger pressure fluctuations, and (3) more frequent pressure fluctuations. These factors combine to result in increased brake fluid agitation, mixing, and circulation. In addition, some systems use low pressure return lines to return

brake fluid to the reservoir further increasing brake fluid circulation. The increased brake fluid mixing and circulation in ABS equipped vehicles will result in faster spreading of environmental contaminants, such as water, salts, and oxidizers (e.g. Oxygen), and more rapid dissemination of corrosion or thermal degradation products throughout the system. This means that corrosion or brake fluid degradation products generated in one part of the system will migrate faster to other parts of the system. Also, environmental species entering at one point of the system can influence performance of other parts of the system. Increased circulation can also accelerate the rate of loss of brake fluid components by evaporation, permeation through seals and hoses, or absorption into polymers. For example, thermal degradation of corrosion inhibitors in a conventional system would primarily influence the rate of corrosion near the wheel cylinders where temperatures and degradation is the greatest, but in an ABS system, the increased brake fluid mixing will result in the corrosion inhibitor concentration of the entire system decreasing faster. In addition, ABS systems use close tolerance valves that must operate quickly and more concisely than conventional braking systems. That is, ABS equipped systems may be more susceptible to degradation in performance due to corrosion or deposits.

NHTSA has examined metallic components removed from ABS systems at their Vehicle Research and Test Center (VRTC) in East Liberty, Ohio. These examinations consisted of visual examination, optical microscopy, and scanning electron microscopy (SEM). The SEM examinations were conducted in conjunction with an energy dispersive spectrometer (EDS) which analyzes the x-rays generated by the electron bombardment in the SEM enabling identification of the elements in the area of the sample being imaged. The results of these examinations were reported to NIST by Jim Hague of VRTC in August of 1997. Their findings are summarized as follows:

(1) visual evidence of corrosion damage is observed on iron alloy components approximately 1/3 of the time (typically no damage is observed to stainless steels),

(2) the damage observed usually consisted of shallow pitting similar to that reported by Jackson et al. [3],

(3) the pits were filled with deposits of varying morphologies,

(4) one deposit variant consisted of a reddish-brown “gel-like” substance (this substance was also observed in conjunction with all of the other morphologies),

(5) frequently, harder particles of another phase were found in this gel,

(6) in most cases when corrosion pits were found on iron, copper deposits of varying morphology were also found,

(7) three different copper deposit morphologies were observed:

    (i) small discrete particles almost spherical in shape ranging in size from 0 μm to 20 μm,

    (ii) a “sponge-like” morphology where it appeared the deposit consisted of two phases one being copper and the other apparently being iron corrosion products, and

    (iii) a large copper particle or “nugget morphology” where it

appeared that either one particle had grown large or several smaller particles had grown together to form a single larger particle.

(8) the small copper particles were found both inside and outside of the shallow pits on the iron,

(9) the copper sponge and the copper nugget morphology were found in the shallow pits associated with and usually under the gel-like substance, and

(10) at the base of the pits the iron was usually smooth and shiny with evidence of etching and crystallographic attack.

2.6 Corrosion Issues and Hypotheses

2.6.1 Copper Deposit Origin and Morphology - The corrosion scenario hypothesized to explain the observations of VRTC is: the copper in the brake lines corrodes at a slow rate over several months or years resulting in copper ions in the brake fluid. These ions then act as oxidizers and plate out in the ABS valves when the corrosion inhibitors can no longer prevent corrosion of the ferrous components. According to this hypothesis, copper corrosion starts when the vehicle is new and proceeds at a rate that is limited by the oxidizer content of the brake fluid, mass transport of this oxidizer, and the effectiveness of the corrosion inhibitors in the brake fluid at retarding copper corrosion. Since copper cannot reduce water, oxygen is the most likely oxidizer responsible for this copper corrosion. This oxygen probably enters the system from the external environment through the seals and through air contact with the fluid in the reservoir. Then, this oxygen makes its way to the brake lines by diffusion, convection, or ABS pumping where it is reduced in support of copper corrosion. Even though copper is in galvanic contact with more active metals, the low conductivity of the brake fluid allows copper corrosion to proceed. While this copper corrosion is in progress, the inhibitor concentration in the brake fluid is also decreasing due to thermal decomposition of the corrosion inhibiting species in the brake fluid. Once the inhibitor concentration decreases to the point where the copper ions can adsorb on the surface of the ferrous alloys, the copper ions will take electrons from the iron atoms on the surface. That is, the copper ions will be displaced from the brake fluid solution by ions of the more active metals in the system such as Fe. This will result in the deposition of copper metal in the brake system. However, because the brake fluid has a low conductivity, these copper deposits will be limited to the component and to the locations on the component where corrosion is occurring. One of the objectives of this work is to examine this hypothesis under controlled laboratory conditions.

2.6.2 Brake Fluid Conductivity - Over a wide range of environments, from soils to high purity water, corrosion rates frequently decrease with decreasing electrolyte conductivity. Electrolyte conductivity influences corrosion rates because it determines the reaction rate as a function of distance between a cathodic site, where oxidizers remove electrons from the surface, to the anodic site, where the metal atoms release their electrons. If electrolyte conductivity is low, energy is lost transporting charge through the electrolyte which slows the reaction rates as the distance of transport through the electrolyte increases. In the extreme case, the oxidizing molecules must come close enough to remove the electrons directly from the oxidized atoms. That is, the rate limiting step in many "real-world" corrosion situations is the rate of transport of oxidizers to sites where they can be reduced. So, lowering the conductivity of the electrolyte and increasing the mass transport required usually lowers corrosion rates. However, corrosion rates are influenced by a host of factors other than electrolyte conductivity, some of which may be more important than

conductivity (e.g. oxidizer content). Corrosion scientists frequently examine electrolyte conductivity first because it is a generic indicator of the relative corrosivity of an environment and because electrical conductivity influences the ability to make electrochemical measurements. Since electrical measurements are quicker, easier, and have higher resolution than gravimetric measurements, electrolyte conductivity is an important issue in measuring and understanding corrosion behavior. As a result, the electrical conductivity of different brake fluids was measured as part of this study.

2.6.3 Electrochemical Characterization - Some of the most effective tools developed to combat corrosion are the electrochemical methods for measuring corrosion rates and quantifying the electrochemical properties of metal surfaces in electrolytes. These techniques enable both the quantification of the influence of environmental parameters on corrosion and the monitoring of changes as environments change. Basically, the ability to measure reaction rates by measuring current instead of using a gravimetric technique enables higher resolutions and avoids the issue of estimating the amount of weight loss by the formation of ions and the amount of weight gain by the formation of corrosion products of unknown stoichiometry. Because these techniques can be so beneficial, experiments were conducted to evaluate the difficulty of applying these techniques to the ABS environment.

3.0 EXPERIMENTAL

3.1 Objectives

The primary objective of this study is to develop a better understanding of corrosion phenomena in this environment. To accomplish this objective, three different types of experiments were conducted: (1) exposure tests, (2) electrolyte conductivity measurements and (3) electrochemical measurements. The objective of the exposure tests was to put iron alloys into representative brake fluid samples containing copper ions and other contaminating species that might be encountered in service and determine if corrosion under these laboratory conditions generates copper deposits with morphologies similar to that reported by VRTC. The objective of the conductivity measurements was to quantify the conductivities of typical brake fluids and the influence of environmental and corrosion product contamination of the conductivity of these fluids. The objective of the electrochemical measurements was to gain an understanding of the electrochemical properties of copper and iron in brake fluid environments in order to determine if these measurements can be used to estimate corrosion rates and develop a better understanding of the factors that influence corrosion rates.

3.2 Brake Fluids

For these experiments, brake fluids were obtained from a variety of sources. However, most of the experiments in this study were conducted with three different brake fluids: (1) an OEM brake fluid, (2) an aftermarket brake fluid, and (3) an uninhibited brake fluid. In addition to these three brake fluids, experiments were conducted on 20 samples of used brake fluid provided by VRTC.

3.2.1 OEM Brake Fluid - For a brake fluid that would represent OEM brake fluids, three 473 mL (16 fl. oz.) cans of brake fluid were purchased from a local GM Parts Department. This brake fluid was identified on the cans as "Delco Supreme 11, Part No. 12377967 Fluid 8.800." The MSDS supplied by GM for this brake fluid is given in the appendix. The blue label on these cans identify this brake fluid as being the revised GM formulation that GM adopted around 1995. Apparently,

GM changed their brake fluid chemistry in 1995 to improve the durability of iron corrosion protection following the work of Jackson et al.[3]. As discussed above, Jackson et al. [3] compared the in-vehicle corrosion behavior of two brake fluids aged in the laboratory to represent 30 months of in-vehicle aging and found corrosion to cast iron wheel cylinders with one of the brake fluids, but not with the other. They reported that this corrosion resembled that observed after several years of in-vehicle use and consisted of rust patches with "deposition of significant levels of copper in the corroded region" [3]. When the present work was initiated, this change in the GM brake fluid chemistry was not known and it was thought that laboratory aging of the brake fluid purchased from the GM Parts Department would be representative of the brake fluid found in vehicles manufactured in the 80's and 90's after about 30 months of service.

A two stage thermal aging process similar to the one developed by Jackson at al.[3] was used to artificially age this fluid and obtain a brake fluid sample representative of that expected in service for the exposure tests. The first stage of this aging process consisted of heating 864 mL of the brake fluid with 36 mL of water added at 130 °C for 20 hrs. in a round bottom flask equipped with a reflux condenser and filled with copper and steel turnings (wool). Air, free of CO_2, was bubbled through this solution continuously during this aging process and the temperature was controlled with a heating mantle and a temperature controller using a PTFE coated temperature sensor which was immersed in the solution. The resulting fluid was filtered and placed into a round bottom flask which was open to the air and heated with the heating mantle and temperature controller at 80 °C for 119 hrs. This procedure deviated from that used by Jackson et al. in that (1) slightly longer aging times were used (130 °C for 20 hrs v. 132 °C for 18 hrs. followed by 80 °C for 119 hrs. v. 80 °C for 64 hrs.) , (2) copper and steel turnings were used instead of copper powder and a cast iron wheel cylinder, (3) a single condenser was used for refluxing the solutions instead of two, (4) water was added to the brake fluid at the start of the aging process, (5) the solution was not stirred continuously during the first stage of the aging process and (6) smaller quantities of fluid were used. All of these changes were made to accommodate facility, equipment, materials, or personnel availability at NIST. This thermally aged brake fluid will be referred to as the "thermally aged OEM brake fluid" throughout the remainder of this report.

3.2.2 Aftermarket Brake Fluid and Uninhibited Brake Fluid - For the aftermarket brake fluid and the uninhibited brake fluid, Union Carbide, a supplier of chemical compounds to GM and other brake fluid manufacturers, agreed to supply two brake fluids: one that represents a typical brake fluid formulation including an additive package with corrosion inhibitors and a second which consisted of the same brake fluid base, but without any additives or inhibitors. Approximately one liter of each of these fluids was sent to NIST identified as "Emkadixol® 310 brake fluid" and "Emkadixol® 310 brake fluid base no inhibitors." The MSDS for these brake fluids is also given in the appendix. The Emkadixol® 310 brake fluid will be referred to as the "aftermarket brake fluid" throughout the remainder of this report while the base for this brake fluid without the additives and corrosion inhibitors will be referred to as the "uninhibited brake fluid base." It should be kept in mind that these two brake fluids are identical except for the additive package which contains corrosion inhibitors.

The aftermarket brake fluid and the uninhibited brake fluid base were not thermally aged for the exposure tests. Instead, these fluids were artificially aged for the exposure tests by passing a current between two copper electrodes. The purpose of this electrochemical aging process was to charge these brake fluids with copper ions in a form and at concentration levels similar to that expected following long term use and corrosion under aggressive conditions in service. The electric potential applied to the electrodes in this process stimulates copper corrosion thus allowing copper ions concentrations in the brake fluids to reach levels representative of years of service in a relatively short time. Of course, these applied currents will also stimulate decomposition of the

brake fluid constituents and contaminants (mostly water) altering the brake fluid chemistry, but it was thought that this approach would yield more representative chemistries than adding a copper salt. Thermal aging to deplete inhibitors was not deemed necessary as it was thought that the uninhibited brake fluid base would be a good indicator of corrosion behavior following inhibitor depletion.

Electrochemical aging was accomplished by placing two copper electrodes into an electrochemical cell containing 100 ml of brake fluid as shown in Figure 3. To represent contamination of the brake fluid, 2 mL of pure water and 1 mL of 1 mol/L NaCl were added to the brake fluids before applying the polarizing current. This quantity of water (0.028 mass fraction) and NaCl (3.3×10^{-4} mass fraction (330 ppm)) are on the high side of that expected in service. A fixed current of 10 mA was passed between the copper electrodes with a galvanostat (a constant current power supply with closed-loop control) while the solution was stirred by a PTFE coated magnetic stir bar. After 5 hours at 10 mA, the current was shut off and the electrodes were allowed to sit in the solution while it was stirred continuously overnight (≈14 hrs). Table IV summarizes the electrochemical aging conditions and additions to the brake fluids for these solutions. The resistivity of the brake fluids increased continuously during this process and, after about 3 hours, 1 mL of pure water and 1 mL of 1 mol/L HCl were added to the uninhibited brake fluid to enable the power supply to keep the current at 10 mA. This second addition was not required for the aftermarket brake fluid and was not made during the charging process. However, after running a set of exposure tests with the aftermarket brake fluid as electrochemically aged, the same exposure tests were repeated after adding 1 mL of pure water and 1 mL of 1 mol/L HCl to yield a brake fluid with a composition closer to that of the electrochemically aged uninhibited brake fluid base and to evaluate the influence of these additions.

3.2.3 Used Brake Fluid Samples - In addition to the three brake fluids described above, 20 samples of used brake fluid removed from ABS systems were sent to NIST by VRTC. These samples were numbered 1 through 20 with no other identifying features. The history of these solutions and the corrosion and morphology observed in the systems the brake fluids came from were not revealed to NIST. These brake fluids were returned to VRTC for further testing at the conclusion of this study.

3.3 Metals

Corrosion measurements were conducted on metal samples of copper and low carbon steel. The material for these samples was obtained from the NIST storeroom. Oxygen free grade copper (99.95% Cu) was used for the copper samples and 1017 steel was used for the steel samples. Two different sample geometries were used: rods and flat strips. The rods were 3.16 mm in diameter and approximately 100 mm long. The rods were ground to a 600 grit finish and a circumferential line was scribed 32 mm from the end of each rod. The rods were cleaned in methanol, weighed, and immersed in the brake fluid up to the scribe line for each experiment. The flat strip samples were approximately 0.5 mm thick, 12 mm wide and 63.5 mm long and they were scribed with a line 25 mm from the one end of the samples. These samples were ground to 600 grit, cleaned in methanol, and immersed up to the scribe lines for the experiments.

3.4 Exposure Tests

The purpose of the exposure tests was to determine if copper deposit morphologies similar to that observed in ABS components by VRTC and in wheel cylinders by Jackson et al. [3] during

in-vehicle tests could be generated by corrosion of iron under controlled conditions in the laboratory. Two different types of exposure tests were conducted: (1) open circuit free corrosion of iron and (2) galvanic corrosion of an Fe-copper couple. These experiments were conducted in the same cell used for electrochemically aging the brake fluids, Figure 3. For the open circuit corrosion of iron experiments, a low carbon steel rod sample was weighed and immersed into the solution up to its scribe line and allowed to freely corrode in the solution for 5 hours (no applied polarizing currents or potentials). Then, this sample was removed, weighed, and examined with an optical microscope and a scanning electron microscope (SEM). For the galvanic corrosion of an Fe-copper couple experiments, a low carbon steel rod and a oxygen free grade copper rod were weighed and immersed up to their scribe lines in the brake fluid environment and coupled together with a shorting wire outside the environment. These two electrodes were allowed to corrode with the shorting wire passing current between them overnight (14±1 hrs.) after which they were removed, weighed, and examined with an optical microscope and an SEM. The three artificially aged brake fluids were used as the environment for these tests: (1) thermally aged OEM brake fluid, (2) electrochemically aged aftermarket brake fluid, and (3) electrochemical aged uninhibited brake fluid base. A fourth set of exposure tests were conducted in the electrochemically aged aftermarket brake fluid after adding 1 mL of pure water and 1 mL of 1 mol/L HCl to yield a brake fluid with a composition closer to that of the electrochemically aged uninhibited brake fluid base.

3.5 Brake Fluid Conductivity Measurements

The conductivity of the brake fluids was determined with a commercial conductivity cell composed of two platinized platinum electrodes approximately 35 mm apart in a glass column 20.7 mm in diameter. The conductivity measurement cell constant for this type of cell is approximately 100 m^{-1} making this cell best suited for mid-range conductivity measurements. For these measurements, 50 mL of the solution to be measured was placed into a large test tube at room temperature (≈22 °C) and the conductivity cell was put into the tube as shown in Figure 4. Aluminum foil was used to reduce evaporative losses during the measurements. Then, the ac resistance between the two electrodes was measured 3 times each at 30 different frequencies between 3 Hz and 3,000 Hz. The solution resistance measured in this way is usually constant over a wide range of frequencies with increasing scatter at the high and low frequencies. The solution resistance was taken as the mean of the measurements between 10 Hz and 1,000 Hz and the standard error was determined from the standard deviation calculated for these measurements. The conductivity cell constant for the conductivity measurement cell was determined using NIST standard reference materials for electrolyte conductivity SRM 3191 (0.01 $S \cdot m^{-1}$ at 25°C) and SRM 3193 (0.1 $S \cdot m^{-1}$ at 25 °C). The cell constant measurements were made at 25 °C by immersing the test tube into a constant temperature water bath. The cell constant for this cell was determined to be 99.7 ±0.95 m^{-1}.

3.6 Electrochemical Measurements

Three different types of electrochemical measurements were made in the brake fluids: (1) open circuit free corrosion potential measurements, (2) polarization measurements, and (3) two electrode ac-impedance measurements. The purpose of these measurements was to determine if electrochemical measurements can be made in this environment, to determine what types of electrochemical measurements can be made, to gather some preliminary information from these measurements, and to analyze this data to determine the usefulness of these measurements. Before most of these measurements could be made, a suitable reference electrode for this environment needed to be developed.

3.6.1 Brake Fluid Reference Electrode - A reference electrode with a potential that is fixed with respect to thermodynamic equilibrium for a chemical reaction in brake fluid was required for making meaningful electrochemical measurements. An electrode of this type enables reproducible potential measurements that can be related to chemical thermodynamics and kinetics. Examination of the literature on reference electrodes indicated that the Ag-AgCl equilibrium has been used successfully as a reference electrode in ethanol, methanol, and other non-aqueous media [7]. As a result, it was decided to attempt to use this equilibrium as a reference in brake fluid. This electrode was assembled by dismantling a commercial Ag-AgCl in aqueous KCl solution reference electrode, removing the KCl solution, regrowing the AgCl layer by polarizing the Ag element in an HCl solution [7], replacing the reference solution with a solution made from 50 mL of the uninhibited brake fluid (no inhibitors) by adding 2 mL of 1.00 mol/L HCl and 1 mL of 10 mol/L LiCl. This electrode and a commercial calomel reference electrode (E=0.242 V vs. saturated hydrogen electrode) were used as reference electrodes in a 0.1 mol/L H_2SO_4 solution and polarization curves were obtained for a Pt sample using both types of electrodes. In these measurements, the Ag-AgCl in brake fluid reference electrode performed satisfactorily and the polarization curves obtained with this electrode were as repeatable as those obtained with the commercial calomel reference electrode. The potential difference between the new electrode and the commercial calomel electrode was estimated by comparing the potential intercepts estimated with linear regression for the Tafel region of hydrogen evolution where the logarithm of the current varies linearly with potential. The difference between the two electrodes estimated in this manner was 0.076 V with the calomel electrode having the higher potential. Then, once it was ascertained that the Ag-AgCl in brake fluid electrode would perform satisfactorily as a reference electrode during dynamic measurements, its potential was measured statically at 25 °C by placing it and two commercial calomel reference electrodes into a beaker immersed in a constant temperature bath held at 25 °C. These measurements indicated that the potential of this electrode would be +0.167 ±0.002 V when measured with a saturated hydrogen electrode as the reference electrode according to IUPAC convention [8].

3.6.2 Corrosion Potential Measurements - The potential of an electrode immersed in an electrolyte is a measure of the chemical energy available in the electrolyte to drive electrochemical reactions (i.e. corrosion) and, since rates are usually related to the driving force, potential is also an indicator of the relative rates of these reactions. Since we can only measure the potential difference between two points in an electrolyte, the potential of an electrode in an electrolyte must be measured by immersing a second electrode into the electrolyte. To enable comparison of the corrosivity of different electrolytes, the potential of this second electrode should be fixed by a single electrochemical reaction (according to the relationship, $\Delta G = -nFE$) and independent of the composition of the electrolyte. In this case, measuring the potential difference between this "reference" electrode and a metal in different electrolytes enables comparison of the chemical driving force available to cause corrosion in the electrolytes though interpretation can become complex (especially in the presence of inhibitors). To evaluate the possibility that an electrochemical sensor could be used to evaluate the corrosivity of different brake fluids, the potential of pure copper and pure iron was measured in samples of brake fluid using the Ag-AgCl in brake fluid reference electrode. This was done by taking either pure iron (0.9999 mass fraction) or oxygen free grade copper (0.9995 mass fraction) and holding it against the outside of the reference electrode as shown in Figure 5. For these measurements, 20 samples of used brake fluid were supplied to NIST in numbered plastic bottles (30 to 50 mL of fluid in each) by VRTC. No information on the history of the samples was provided to NIST, but VRTC has this information and at the completion of these measurements the samples were returned to VRTC for additional testing. These samples varied significantly in color (from almost clear to brown or green) and some contained what appeared to be corrosion products in the bottom of some of the vials. To make

these measurements, the electrode pair was inserted into the container holding the brake fluid, held in place, and continuously monitored until a steady potential was reached. The potentials were measured with the Ag/AgCl in brake fluid reference electrode connected to the ground or low connection of a high input impedance digital voltmeter and the sample of either copper or iron connected to the high lead in accordance with IUPAC convention[8]. This steady state potential was then recorded as the "corrosion potential" for the metal in the brake fluid and the standard deviation of the measurements after steady state was reached was used as an estimate of the uncertainty in the measured value.

3.6.3 Electrochemical Polarization Measurements - Electrochemical measurements of the polarization behavior of the brake fluids were attempted using an electrochemical cell similar to that illustrated in Figure 3 with the inclusion of the brake fluid reference electrode, a Luggin capillary, which acts as a salt bridge between the reference electrode and the sample, and by replacing one of the samples with a Pt counter electrode. For these experiments, the solutions were deaerated by bubbling nitrogen gas through them and the potential was controlled with a potentiostat which is a high-gain closed-loop amplifier for maintaining the potential difference between the reference electrode and the sample constant or varying in some predetermined manner. In this case, the potential was swept at constant rates and the corresponding current required to maintain the potential at the desired value recorded, creating a polarization curve of current as a function of potential. Initially, the conductivity of the electrolyte was so low that closed loop control was not possible, but modifications were made to enable measurements. However, electrolyte resistance will still create a measurement error in the potential of the sample (the "IR" error) which requires correction for conductivities this low and the current interrupt technique for IR correction was attempted.

3.6.4 Two Electrode AC-Impedance Measurements - The purpose of conducting 2 electrode ac-impedance measurements is to see if this technique can be used to determine the corrosion rate of copper and steel in brake fluids. For these measurements, two flat sheet samples of the metal whose corrosion rate was to be determined, were immersed up to their scribe lines in 50 mL of the brake fluid 10 mm apart as shown in Figure 6. Then, the impedance of this cell was measured at frequencies from 0.05 Hz to 5,000 Hz using a computer controlled potentiostat with a frequency response analyzer.

4.0 RESULTS

4.1 Exposure Tests

Two types of exposure tests, free corrosion of a low carbon steel rod and galvanic corrosion of a low carbon steel rod coupled to an oxygen free grade copper rod of the same size, were conducted in the three artificially aged brake fluids.

4.1.1 Thermally Aged OEM Brake Fluid - Figure 7 is an optical micrograph of the corrosion observed on the steel rod after exposure to the thermally aged OEM brake fluid for 5 hours at room temperature. An unattacked area can be seen at the left side of this figure. Clearly, this solution contained enough oxidizer that visible attack could occur in this relatively short time. Figure 8 shows this same sample at a higher magnification and in this micrograph it can be seen that the corrosion appears to be localized into shallow pits or grooves. Figure 9 is an SEM micrograph of two of these areas of localized attack. In this figure, it can be seen that the attack morphology is indeed pit-like and it appears deeper than indicated by the optical micrographs. There is little evidence of deposition of corrosion products or of reduced oxidizers. Also, it appears that the

grooves are the result of the pits spreading laterally in one direction much faster than in the other directions. The preferred growth direction does not appear to be related to the scratches left on the surface from the 600 grit finish, but this possibility should not be ruled out as the evidence may have been removed by corrosion. Figure 10 is an EDS spectrum taken in the SEM from this sample with the locations of the X-ray energy peaks expected for Cu, Si, Cl, Mn, and Fe indicated. This figure shows no evidence of deposition of an oxidizing element on the surface supporting the evidence in the SEM image.

4.1.2 Electrochemically Aged Aftermarket Brake Fluid - The same exposure tests were conducted on the aftermarket brake fluid after it was electrochemically aged to charge the fluid with copper ions. Figure 11 is an optical micrograph of the steel rod exposed to this solution coupled to a copper rod for 13 hours. In this figure, the sample appears to be virtually unattacked by this environment and exposure conditions except for a small number of dark spots. Examination of this sample in the SEM, Figures 12 and 13, revealed that the dark spots seen in the optical image were indeed small areas of corrosion. After the addition of 1 mL of pure water and 1 mL of HCl to this brake fluid, considerably more corrosion resulted during the exposure tests as shown in the optical micrograph of Figure 14 and the scanning electron micrograph of Figure 15. In these figures, two types of pits can be seen: (1) pits filled with white (in the SEM) deposits, and (2) shallow deposit-free pits. Figure 16 is an SEM micrograph of the bottom of one of these shallow pits and, from this figure, it appears that this surface is covered with smaller hemispherical pits about 0.3 μm to 0.5 μm in diameter. Figure 17 is an EDS spectrum from one of these pits and there is a slight indication of copper present in this area while there is no such evidence outside the pit. The EDS spectrum obtained from the whitish deposit in the pit shown in Figure 11 is shown in Figure 18 and this spectrum shows no evidence of copper in this deposit which appears to be corrosion products.

4.1.3 Electrochemically Aged Uninhibited Brake Fluid - The same exposure tests were conducted in the electrochemically aged uninhibited brake fluid. Figure 19 is an optical micrograph of the corrosion and deposits found on the surface of a steel sample after corroding freely for 5 hours in this environment. Three almost circular pits can be seen in this figure that range in size from about 8 μm to 22 μm. A deposit can be seen inside these pits and this deposit was red in color. Around the outside of the pits, the surface is darker in color than the remainder of the unattacked surface. These "halos" of dark color extend from the edge of the pit out approximately the diameter of the pit to the point where they become lighter and fade into the unattacked surface. Judging from a similar looking small stain along the left edge of this figure, a small pit is probably located at the center of this stain inside the scratch which intersects the stain. Figure 20 is a scanning electron micrograph of a representative pit in the surface of this sample. No features or deposits that could be responsible for the dark color of the "halos" around the pits can be seen in this figure. The pit in this figure is about 45 μm in diameter and the deposit in this pit can be seen to consist of a large number of smaller particles which are shown at higher magnification in Figure 21. While the smaller particles appear almost spherical in this figure, the larger particles are generally elongated in one dimension. Examining these particles closer indicates that some of the large particles appear to be composed of one or more particles that have grown together. In addition, it appears that many of the smaller particles nucleated and grew on the surface of the larger particles and some of these particles have facets that appear to have 3 or 6 fold symmetry. Looking between these particles some regions of a phase that looks amorphous (smooth and featureless) can be seen. Figure 22 is an EDS spectrum taken from the deposits inside one of the pits in this sample and Figure 23 is an similar spectrum taken from the unattacked surface of the sample far enough away from pits to avoid fluorescence from the elements in the deposits. By comparing these two spectra, it can be seen that only two elements appear to be present in the area of the deposit, iron and Cu, while only iron is present in the spectrum taken away from the deposit. That is, copper was the dominant element in the deposit with its peaks being roughly 5 times the size of the equivalent peaks from Fe.

On the other hand, no evidence of copper or any element other than iron could be detected above the background level in the spectrum obtained from the unattacked surface.

Figure 24 is an optical micrograph of a steel sample corroded in the same solution galvanically coupled to a copper sample overnight. In this figure, a large patch of deposits that is larger in diameter than the horizontal dimension of the figure can be seen. This patch of deposits is about 200 μm in diameter and the central region, where the deposits appears continuous in this figure, is about 120 μm in diameter. This deposit was red in color similar to the deposits in the pits shown in Figure 19 and the surface of this sample was covered with a number of these deposits some of which fell off while the sample was being removed and cleaned in methanol. Figure 25 is a low magnification scanning electron micrograph of one of these large deposit patches and several smaller ones can also be seen in this figure. The large patch of deposits in this figure is about 400 μm across and about 800 μm long. The deposits in this patch can be seen at higher magnification in Figure 26. In this figure, the particles are clearly smaller than those shown in Figure 21 which is at the same magnification, and more of the featureless amorphous phase can be seen. The EDS spectrum from this sample was essentially identical to those obtained from the other sample corroded in this solution. That is, copper and iron peaks were observed in the deposits while only iron was observed on the unattacked surface as shown in Figures 22 and 23.

4.2 Brake Fluid Conductivity Measurements

The conductivity of the brake fluids was measured in four conditions: (1) as-received or "neat," (2) with 1 mL of pure water added (2% by volume), (3) with 1 mL of water and 1 mL of 1 mol/L NaCl added, and (4) artificially aged for the exposure tests (and after the test were completed). Table V contains the results of these measurements. By examining this table it can be seen the conductivity of these solution varied by more than 2 orders of magnitude. The lowest conductivity was observed for the uninhibited brake fluid base without any additions. The as-received conductivities of the other brake fluids were more than 25 times that of the uninhibited base. Adding water to this brake fluid increased the conductivity by about 50%, but adding NaCl to this fluid increased the conductivity by 2 orders of magnitude. Similar, though not as dramatic, changes were observed for the other brake fluids.

4.3 Electrochemical Measurements

To evaluate the possibility of using electrochemical measurements to measure and understand corrosion in this environment, three different types of electrochemical measurements were made: (1) open circuit potential measurements, (2) electrochemical polarization, and (3) two electrode ac impedance.

4.3.1 Open Circuit Free Corrosion Potential Measurements - Table VI contains the results of the open circuit or free corrosion potential measurements for oxygen free grade copper and pure iron in the 20 samples of used brake fluid sent to NIST by VRTC. Included with these measurements are identical measurements conducted in the three solutions used for the exposure tests of this study. By examining this table it can be seen that there is no clear trend and the potentials appear to be randomly distributed. However, by examining the measurement for the artificially aged solutions used for the exposure tests of this study it can be seen that the potentials for these solutions were in the low end of the range especially for sample 23 which is the artificially aged aftermarket brake fluid, but this measurement was made following the addition of 1 mL of water and 1 mL of 1 mol/L of HCl to this solution. Since this addition had been made after the electrochemical aging process and the exposure tests, this fluid probably contained considerably more hydrogen ions than any of the other fluids.

4.3.2 Electrochemical Polarization Measurements - A number of electrochemical polarization experiments were conducted using the Ag/AgCl in brake fluid reference electrode. However, satisfactory and reproducible results were not obtained for any of the IR compensation techniques attempted in the time frame of this study. The authors would like to point out that measurements have been made in our laboratory in solutions with lower conductivities than these, but that development and optimization of a measurement method and obtaining enough results to be certain of the validity of the results is beyond the scope of the present program.

4.3.3 Two Electrode AC Impedance - The two electrode AC impedance technique was attempted because it frequently enables measurements in low conductivity solutions. This measurement method obtains a polarization or charge transfer resistance which is inversely proportional to the corrosion rate. Translation of these measurements to an actual corrosion rate requires determination of the proportionality constant relating the reciprocal of the charge transfer resistance to the corrosion rate. Determination of this proportionality constant can be accomplished through electrochemical polarization measurements or it can be estimated by making assumptions about the corrosion mechanism and the electrochemical kinetics of the system. However, these constants should not change significantly for small changes in solution chemistry. Therefore, comparison of the reciprocal of the measured charge transfer resistance is a good indicator of the influence of changes in electrolyte chemistry on corrosion rates. As a result, the reciprocal of the charge transfer resistance as estimated from the impedance data for copper and iron in different brake fluid mixtures is presented in Table VII and in graphical form in Figures 27 and 28. By examining this table and the figures, it can be seen that, unlike iron, the corrosion rate of copper does not increase significantly when water is added to the brake fluid. Also, adding NaCl to the brake fluid-water mixtures significantly increased the corrosion rates for both copper and iron. The inhibitors in the aftermarket and in the OEM brake fluids significantly reduced the corrosion rate increases seen with the addition of water and NaCl.

5.0 DISCUSSION

The corrosion scenario hypothesized to explain the observations of VRTC is that the copper in the brake lines corrodes at a slow rate over several months or years resulting in copper ions in the brake fluid which then act as oxidizers and plate out in the ABS valves when the corrosion inhibitors can no longer prevent corrosion of the ferrous components. This hypothesis actually consists of five separate issues: (1) copper corrosion in brake fluid, (2) transport of copper ions to the ABS valves, (3) depletion of the protective inhibitors, (4) displacement of copper ions from the solution by iron ions, and (5) copper deposit morphology.

By comparing the rates of corrosion for copper and iron in the uninhibited brake fluid base to those in the aftermarket brake fluid in Table VII, it can be seen that the corrosion inhibitors in the aftermarket brake fluid lower the corrosion rates of both copper and iron and, in fact, the copper corrosion rate is reduced to a much greater extent than the rate of iron corrosion. However, the copper corrosion rate is still about an order of magnitude greater than the measurement error indicating that the corrosion rate of this metal is still significantly greater than zero in this brake fluid. Similar numbers are observed in this table for the OEM brake fluid. That is, while the corrosion rate of copper is lowered significantly by the addition of the inhibitors, copper is still corroding. This is not surprising because copper is not thermodynamically stable in this environment (aerated brake fluid) and inhibitors do not alter these thermodynamics. Corrosion inhibitors reduce corrosion rates by slowing the rate determining step in either the anodic or the cathodic reaction. Inhibitors of the type used in brake fluids (mostly amines) accomplish this by

forming a layer of adsorbed molecules on the surface of the metal that inhibits mass transport to the metal surface. As illustrated graphically in Figure 29, if an inhibitor slows the anodic reaction (oxidation of the metal), then the steady state free corrosion potential of the corroding electrode will increase and, if the inhibitor slows the cathodic reaction (reduction of an oxidizing agent), the potential of the corroding electrode will increase. This is why it was thought that the open circuit free corrosion potential measurements might be a means of measuring or detecting inhibitor depletion.

If it is assumed that the chemical constituents of the brake fluid base act as inert diluents with no influence on the chemical thermodynamics of copper corrosion, then copper corrosion in this environment can be analyzed in terms of chemical and electrochemical reactions between water, copper, and oxygen. This is a reasonable first order approximation given the observations of this study, but it assumes that the copper ion solubility is not limited by the brake fluid. Even though glycols have relatively high solubilities for an organic solvent, the validity of this assumption will be limited by the solubility of these ions in the brake fluid. One convenient manner of examining electrochemical equilibria in aqueous solutions was advanced by Pourbaix and co-workers [9] and that is the electrochemical equilibrium diagram or "E-pH" diagram. Figure 30 is an electrochemical equilibrium diagram for the copper-water system where the potential axis has been adjusted to correspond to potentials measured with the Ag-AgCl in brake fluid reference electrode used in this study (E=0.167 V vs. SHE). In this diagram, the dotted lines represent the predominance boundaries between ions in the solution (the equilibrium point for equal concentrations) and the solid lines represent the stability boundaries between solid phases or between a solid phase and the solution for a concentration of the metal ions in the solution of 1 $x10^{-6}$ mol/L (The metal ion concentration in this diagram is noted as pM=6, where pM = -log (metal ion concentration) analogous to pH for hydrogen ion concentration [10]). The stable phase in each region is identified in bold face and the predominant ion in plain face. Regions where a solid phase is not stable are labeled "Corrosion" as these are the regions where corrosion will be the most severe. The numbers on the lines identify the reactions which the lines represent and the reactions with the calculations for this diagram are given in Appendix C.

This diagram was calculated, as is normally the case in aqueous corrosion, by assuming the concentration of water is approximately one. However, in brake fluid the concentration or activity of water is considerably less than unity. As a result, this diagram was re-calculated with the activity of water adjusted to 0.01 to represent a brake fluid containing approximately 0.01 mass fraction water. The resulting diagram is given in Figure 31 and by comparing this figure to Figure 30, it can be seen that lowering the activity of water resulted in shifting the lines that represent reactions involving water while the reactions that do not incorporate water remained stationary. By examining the pH range expected in brake fluids given in Table III and the range of copper potential measurements in the used brake fluid samples given in Table VI, it can be seen that these calculations indicate that the potential of the pure copper wire in the measurements was close to the equilibrium line between copper metal and cuprous oxide (Cu_2O) in a region where the dominant ion should be the cuprous ion (Cu^{+1}). By examining Table VIII which is a compilation of the ions and solid phases in the copper-water system and their colors, it can be seen that the cuprous ion is colorless and that the hydrated form of cuprous oxide ($Cu_2O \bullet H_2O$ or Cu(OH)) is yellow. This seems surprising since the used brake fluid samples were brown or green in color, but keep in mind that the copper wire used for these measurements was freshly ground with 600 grit sandpaper immediately before immersion in the sample. As a result, the initial potential should be in the copper metal region of Figure 31. If an oxidizer is present in the environment which can be reduced at this potential, then it will take electrons from the copper surface. Copper will attempt to replace these electrons by corroding. If the rate of electron removal (reduction) is greater than the rate of replacing them by oxidation, then the potential of the electrode will increase, but increasing

the potential will increase the rates of oxidation reactions while slowing the reduction reactions. As a result, the potential of the copper electrode will increase until the rate of generating electrons by oxidation of the copper atoms is equal to the rate of removing electrons by reducing the oxidizer. By beginning in the copper metal region in Figure 31 and increasing the potential it can be seen that the first anodic reaction in this diagram that will retard or stop the rise in potential of a copper electrode is reaction #7 (as listed in Appendix C)

$$2Cu + H_2O = Cu_2O + 2H^+ + 2e^- \quad (1)$$

for fresh inhibited brake fluid and reaction #15

$$Cu = Cu^{+2} + 2e^- \quad (2)$$

for uninhibited or inhibitor depleted brake fluid. So, it is reasonable to assume that the open circuit free corrosion potential for most if not all of the measurements given in Table VI are measurements of the equilibrium potential for reaction #7 and that the variations in the measurements come from four sources: (1) variations in the water content of the brake fluid, (2) variations in the pH of the brake fluid, (3) variations in the oxidizer content, and (4) measurement errors.

The most interesting result of this analysis is not an explanation of the meaning of the copper open circuit free corrosion potential measurements, but an understanding of the role of the water content of the brake fluid on corrosion of copper in this environment. First, the energy available from corrosion of copper is insufficient to reduce water as illustrated by the potentials in Figure 31. Potentials below -0.3 V in this figure would be required to reduce water and evolve hydrogen gas even at the lowest pH. That is, neither water nor hydrogen ions (low pH) can cause corrosion of copper in this environment. As a result, some other species must be acting as the oxidizer that promotes copper dissolution in this environment. This is not surprising as the same is true for copper in aqueous solutions, Figure 30. The most likely oxidizer is oxygen coming from air contact with the fluid in the reservoir and spreading through the brake lines by the pumping action of the ABS system. More importantly, these calculations indicate that if water is present it should react with the copper ions in the solution and precipitate out as either cupric or cuprous oxide (or hydroxide) lowering the pH according to reactions of the form

$$Cu^{+2} + H_2O = CuO + 2H^+ \quad (3)$$

which is reaction #11 in Figures 28 and 29, and react with copper metal according to reaction #7 (eq. (1) above) which is the copper passivation reaction. That is, adding water to brake fluid without copper ions in it will be beneficial as it will promote the formation of protective copper oxides and hydroxides on the surface of copper possibly resulting in passivity and a corrosion rate approaching zero. However, adding water to brake fluid with copper ions in it will cause the precipitation of copper oxides and hydroxides from the brake fluid solution with the production of hydrogen ions that will lower the pH of the brake fluid solution. Of course, the buffer capacity of the inhibitor package added to the brake fluid will initially prevent the pH from changing, but once the buffer capacity is exceeded, which will happen first in occluded and stagnant regions such as crevices where these precipitates may accumulate, the pH of the brake fluid will decrease increasing the solubility of copper and iron ions in the solution and accelerating corrosion. Once the pH gets low enough that iron oxides and hydroxides can no longer form on the surface of the iron components and protect then from further attack, these components will corrode by reducing copper ions and hydrogen ions from the solution. Originally, it was thought that the white gel-like deposits reported by VRTC were going to be ferrous hydroxide ($Fe(OH)_2$) which is white and will also produce acidifying hydrogen ions when it precipitates by reaction between ferrous ions and water,

but now it appears that these deposits may be a combination of copper and iron hydroxides.

The corrosion scenario needs to be modified slightly to include the role of copper ion precipitation in occluded or stagnant regions such as ABS valves and crevice regions in these valves and other locations. That is, when fresh, water-free brake fluid is put into a vehicle, the solubility of copper ions will be limited by their solubility in the brake fluid base constituents. Then, as the brake fluid absorbs water, the solubility of the copper ions will be reduced, assuming that the solubility of the copper ions is greater in the brake fluid than in water, which will result in the precipitation of copper oxides or hydroxides and the production of hydrogen ions which lower the pH. If this occurs in an occluded region such as crevices in an ABS valve (or at stagnant locations on the exposure tests samples), then the local chemistry of this region can become depleted in inhibitors and the buffer capacity exceeded, lowering pH and causing corrosion of iron components in this region. In other words, precipitation of copper ions as copper hydroxides in crevices as the water content of the brake fluid increases can stimulate attack of the iron components. Once iron corrosion starts producing iron ions, these ions can also react with water to form hydroxides and lower the pH, but the copper reaction is such that a lower pH will result for the same ion concentration. As a result, iron hydroxide precipitation will tend to occur on the outside of the copper hydroxide gel. This postulate would result in localized regions of attack that appear like calcareous deposits with an outer shell of iron oxides and hydroxides covering shallow pits that contain copper hydroxide gel and metallic copper particles. Since the pH inside the deposit is lower than the pH outside the deposit, the inside wall of the shell has a higher iron ion concentration in equilibrium with it than the outside wall so, the deposit grows larger as corrosion proceeds.

The cathodic reactions supporting iron corrosion in these calcareous deposits will be oxygen reduction, hydrogen ion reduction, and copper ion reduction. The driving force for reduction of hydrogen ions is not very great for iron corrosion at pH's above 8 or 9 so the rate of this reaction will be quite slow. The oxygen content of the brake fluid is not very high and, since the conductivity of the brake fluid is low, the oxygen must permeate through the gels to contribute significantly to corrosion rates. As a result, copper ion reduction will be the primary cathodic reaction, but will be limited to the inside of the deposit (or immediately adjacent to the deposit) by the low conductivity of the brake fluid. This will result in the formation of copper metal deposits inside the corrosion deposits on the iron surface. The nucleation and growth of copper metal will reduce the copper ion concentration inside the deposit, but these ions will be replaced by copper ions coming from the copper hydroxide gels or permeating through the outer "shell" of the deposit. So, as corrosion propagates, the copper hydroxide becomes replaced by iron hydroxide, iron oxides, and particles of copper metal. If one of these particles of copper metal becomes detached from the surface of the corroding iron, it will stop growing and may even start to corrode if oxygen reaches it, but it could also start growing again if it comes into physical contact with the corroding surface or another copper particle in contact with the corroding surface. As long as one of these copper particles is in physical contact with the corroding iron, they all will continue to grow. The rate of growth will be determined by the iron corrosion reaction, the copper ion concentration (pH), and the distance that charge must be transported through the low conductivity electrolyte. The low conductivity of the brake fluid is what limits the cathodic reaction to the inside of the deposit. Otherwise, copper deposits would be found all over the sample. Inside the deposit, the charge carrier density in the electrolyte is orders of magnitude greater than it is outside the deposit due to the lower pH (and the resulting greater ion solubilities) and the iron ions being generated by corrosion. As a result, the conductivity barrier inside the deposit is orders of magnitude less than it is outside the deposit. In addition, low electrolyte conductivity does not limit particle growth, it promotes growth in directions that minimize ionic path length over growth in directions that maximize the surface area and the rate of copper ion mass transport with no regard to ionic path lengths. Looking at the deposits in Figures 21 and 26, these particles do not appear to be growing

in directions that minimize ionic transport distances (in the plane of the underlying iron). Instead, they appear to be growing in all directions including away from the corroding surface and over the top of other copper particles. That is, the availability of copper ions seems to be the determining factor in the growth of these particles not ionic path length. In addition, it is clear from these figures that galvanic coupling the steel sample to a copper rod 30 mm away and the longer exposure time resulted in significantly more copper deposited, but it also resulted in smaller copper particles in the deposits. The primary factors that limit copper grain size is the nucleation rate which is determined by the overpotential (the thermodynamic driving force), the availability of copper ions (mass transport rates), the extent of iron corrosion, and the size of the deposit. Clearly, the copper rod 30 mm away managed to increase the overpotential driving copper particle nucleation and growth. Since the copper particles could also grow together to make a polycrystalline solid, as usually occurs during plating, it is concluded that copper particle size is limited by the extent of corrosion, the corrosion deposit size, and the stochastic processes occurring inside the deposit.

To examine copper ion equilibria in brake fluids further, two copper electrodes were immersed in a beaker with about 50 mL of the aftermarket brake fluid. The first concern was the green color of the copper charged brake fluid solutions used in this study as compared to the colors expected for copper ions and phases, Table VIII, which are mostly blue. Since copper chloride is green, it was postulated that the green color of the solutions used for the exposure tests of this study and in the used brake fluid samples might be the results of copper chloride complexes in these brake fluids. As a result, nothing was added to this brake fluid and a current was passed between the electrodes for an hour while a sheet of white paper was placed behind the beaker and the color of the solution observed by eye. A stir bar was added to the solution and the solution was stirred periodically. Upon switching on the current, a green color was observed to form in the solution adjacent to the anode. This green layer thickened and began streaming down the sample. After a few minutes, the stirrer was switched on and the solution turned green. As this continued, the solution became greener, but when the stirrer was turned off and the layer on the anode allowed to reform, the color of this layer appeared to be a bluish-green. After an hour of charging with this current, the entire solution became this blue-green color. Then, the solution was left in the beaker open to lab air overnight. The next morning a whitish gel-like precipitate was observed floating in the lower half of the solution in the beaker and the solution above this layer was green with significantly less blue tint to it. This precipitate was filtered out and the beaker left out overnight again. The next morning more precipitate was found in the solution and the remaining solution was a lighter green. This process was repeated periodically over the next month and the precipitate continued to form as the brake fluid presumably absorbed more moisture from the air until the color of the filtered solution was almost the same color as that of the brake fluid remaining in the storage container. The conclusion is that the gel-like precipitate that appeared whitish in the green solution and green in the filter paper is a mixture of cuprous hydroxide ($Cu_2O{\bullet}H_2O$ or Cu(OH)) which is yellow and cupric hydroxide ($CuO{\bullet}H_2O$ or $Cu(OH)_2$) which is light blue. Mixing a yellow phase and a blue phase yields a green colored precipitate. Similarly, putting a colorless cuprous ion and a light blue cupric ion in a yellow, tan, or brown solution will yield a green colored solution until the concentration of the blue cupric ion becomes great enough to shift the color to the point where the solution can be considered blue. Therefore, it is concluded that the green color in the solutions is the result of mixing blue and yellow and, since the used brake fluid samples were similarly colored, the green color of the electrochemically aged solutions is not an indication that these solutions contain unrepresentative copper chloride complexes. These observations are also consistent with the hypothesis that increasing the water content of a brake fluid lowers the copper ion solubility.

The electrochemically aged solutions did contain chloride ions and at levels above that expected in service. Also, copper does form complexes with the chloride ion. Copper also forms

complexes with other species and these complexes can have a dramatic effect on corrosion thermodynamics and kinetics. However, the results of these experiments are consistent with the assumption that the brake fluid base acts as a inert diluent. If this is the case, the chloride ion accelerates corrosion in two ways. First, it competes with the inhibitors for sites on the surface of the metals in the solution effectively increasing the concentration of inhibitor required to block active surface sites and prevent corrosion. In other words, it reduces the amount of inhibitor depletion required before corrosion can start. Second, it accelerates corrosion by destabilizing protective layers and can cause pitting in passivated systems. However, if the mechanism of corrosion was changed by the higher chloride level in the fluids used for these exposures tests, it would be obvious from the morphology of the corrosion damage. Since this is not the case here, it will be assumed that the high level of chlorides used in these experiments served only to accelerate attack and did not modify the mechanism of attack.

Finally, the standard corrosion test for brake fluids in the Code of Federal Regulations (49 CFR 571.116) involves adding 5% by volume water to fresh brake fluid into a container, immersing coupons of the various metals to be evaluated, and then sealing this container. As pointed out above, adding water to fresh brake fluid before immersing copper samples into it will probably result in passivating the copper surface resulting in much lower corrosion rates than may occur in service. In fact, small amounts of water are frequently added to organic solvents to inhibit corrosion [11]. Also, sealing the container will limit the oxygen available to act as an oxidizer and cause corrosion of copper. However, the corrosion scenario examined in this work, and modified in this discussion, incorporates copper corrosion in brake fluids with low water content followed by precipitation of these copper ions in occluded locations with limited transport as the water content increases. This process could result in the inhibitor and buffer capacities of the fluid becoming exceeded locally and localized attack. The existing standard tests do not evaluate the potential for this attack. While these brake fluids and standard tests have served this industry for a number of years, changes in brake system designs including ABS systems may put greater demands on these fluids. The increased brake fluid mixing found in ABS equipped vehicles will promote the transport of oxygen absorbed from air to the copper metal in the brake lines where it will act as an oxidizer promoting copper corrosion. In the existing standard test, the container is sealed with a small air space above the fluid for the duration of the exposure. As a result, the existing standard test method is not representative of the corrosion conditions that may exist in these systems. A similar conclusion was reached by Jackson et al. [3] about the ability of the existing standard corrosion test method to evaluate the corrosivity of brake fluids after long term vehicle use.

6.0 CONCLUSIONS

The hypothesis that the large surface area of copper in the brake lines corrodes slowly during normal service resulting in the accumulation of copper ions in the brake fluid that can be transported to other parts of the braking system and cause corrosion of ferrous alloys, once the corrosion inhibitors become depleted, was evaluated by conducting exposure tests in brake fluids artificially charged with copper ions. The results of the exposure tests are consistent with this hypothesis. The largest copper particles observed during this work were about 8 μm in diameter following only 5 hours of exposure. The results indicate that there is no physical reason why longer exposures will not result in larger particles.

Electrochemical measurements were conducted to evaluate the difficulty of conducting electrochemical measurements of corrosion rates in the ABS brake fluid environment. While the low conductivity of these fluids is low enough to inhibit the application of the methods, it is concluded that electrochemical measurements can be used to study the electrochemical properties of metals in these fluids, measure corrosion rates, and evaluate the effect of changes in chemistry and time on the corrosivity of these fluids, but the special methods and techniques developed for use in low conductivity electrolytes need to be used to compensate for the errors that result from the low conductivity of the electrolyte.

The analysis of the results of this work indicated that exposure tests conducted in sealed containers of fresh brake fluids with 5% by volume water added prior to testing are not representative of in-service corrosion conditions. Adding water prior to immersion of the coupons will result in passivation of the copper coupons on immersion and excluding air during the exposure test eliminates the oxidizer which can cause corrosion of copper. These two features of the standard corrosion test should result in corrosion measurements that are lower than those that can occur in-service.

ACKNOWLEDGEMENTS

The authors would like to acknowledge the following individuals: G. Person of NHTSA, R. Boyd of NHTSA, J. Hinch of NHTSA, J. Hague of VRTC, P. Levesque of Union Carbide, and F. Wagner of GM. The comments, help, advice, and criticisms of these individuals contributed greatly to the experimental plan and the analysis of the results of this program. The authors would also like to acknowledge the assistance in the laboratory of R. D. Schmidt of the Technical University of Denmark and NIST guest worker.

REFERENCES

[1] Anon., in *Code of Federal Regulations, Title 49-Transportation, Chapter V-National Highway Traffic Safety Administration (DOT) , Part 571-Federal Motor Vehicle Safety Standards*, B. Swidal Ed., Office of the Federal Register, Washington, DC, 1995, pp. 349.

[2] Anon., in *SAE Handbook*, SAE Intl., NY, 1995, pp.

[3] Jackson, G. L., Levesque, R. and Wagner, F. T., Improved Methods for Testing the Durability of Corrosion Protection in Brake Fluids, SAE International Congress & Exposition, SAE Intl., SAE 971007, Corrosion Prevention SP-1265, 1997.

[4] Hellmann, R. H., What the Brake Engineer Wants from Brake Fluid, International Automotive Engineering Congress, SAE, SAE Paper No. 690222, 1969.

[5] Rabold, G. P., Conventional Brake Fluids - State of the Art, Passenger Car Meeting, SAE, SAE Paper No. 780662, 1978.

[6] Jacobson, M. A., Corrosion of Motor Vehicles: Safety and Environmental Factors: The User's View, Corrosion of Motor Vehicles, The Institution of Mechanical Engineers, Conf. Publ. 16, 1974.

[7] Ives, D. J. g. and Janz, G. J., *Reference Electrodes Theory and Practice,* Academic Press, New York, 1961.

[8] Bockris, J. O. M. and Reddy, A. K. N., *Modern Electrochemistry,* Plenum, New York, 1977.

[9] Pourbaix, M., *Atlas of Electrochemical Equilibria in Aqueous Solutions,* NACE Intl., Houston, TX, 1974.

[10] Perrin, D. D. and Dempsey, B., *Buffers for pH and Metal Ion Control,* Chapman and Hall, London, 1974.

[11] Dillon, C. P., *Matls. Perf.*, Vol. No. 11, 1990, pp. 51.

Table I

Maximum permissible mass changes per unit area of exposed surface for brake fluid in the corrosion test specified in Federal Motor Vehicle Safety Standard Number 116 and the corresponding average corrosion rates. The mass changes and corrosion rates measured in this test by Jackson et al. for a high quality brake fluid base without corrosion inhibiting additives is included in this table showing that corrosion inhibitors are not required to pass the corrosion requirements of this standard.

Test Strip Material	**Maximum Permissible Mass Change per Unit Area ($g \cdot m^{-2}$)**	**Corresponding Mean Corrosion Rate ($g \cdot m^{-2} \cdot d^{-1}$)**	**Measured Mass Change for a Brake Fluid Base ($g \cdot m^{-2}$)**	**Measured Mean Corrosion Rate* ($g \cdot m^{-2} \cdot d^{-1}$)**
Copper	±4	0.8	0.0	0.00
Brass	±4	0.8	-0.2	0.04
Cast Iron	±2	0.4	0.0	0.00
Aluminum	±1	0.2	0.1	-0.02
Steel	±2	0.4	-0.4	0.08
Tinned Iron	±2	0.4	2.0	-0.40

* Note, a negative mass change corresponds to a positive corrosion rate.

Table II

List of Compounds found in hydraulic brake fluids compiled from
Material Safety and Data Sheet information obtained from 6 different brake fluid suppliers.

Compound Name on MSDS	Compound CAS Number
Glycol Ethers	989902339
Diethylene Glycol Ethyl Ether	111-90-0
Diethylene Glycol Methyl Ether	111-77-3
Diethylene Glycol Monobutyl Ether	112-34-5
Diethylene Glycol Monopropyl Ether	6881-94-3
Triethylene Glycol Ethyl Ether	112-50-5
Triethylene Glycol Methyl Ether	112-35-6
Triethylene Glycol Monobutyl Ether	143-22-6
Ethylene Glycol	112-27-6
Diethylene Glycol	111-46-6
Triethylene Glycol	107-21-1
Ethylene Oxide-Propylene Oxide Polymer	9038-95-3
Glycol Heavies	25322-68-3
Mixed Proplyene Glycol Lubricants	989953016
Polyalkylene Glycol Lubricant	989916176
Polyethylene Glycol	25322-68-3
Polyethylene Glycol Hexyl Ether	112-59-4
Polyethylene Glycol Monobutyl Ether	9004-77-7
Polyethylene Glycol Monomethyl Ether	9004-74-4
Proprietary Mix of Corrosion Inhibitors	N/A

Table III

Physical properties reported on Material Safety and Data Sheets
for brake fluid from 6 different brake fluid suppliers.

Supplier No.	Boiling Point (° C)	Density (kg/L)	pH
1	227	1.035±.005	10.0±0.5
2	221	1.03	N/A
3†	232	1.026	10.3
4	205	1.036	N/A
5*	260	1.039	9
6	232	0.95-1.00	8.5-10.0

† OEM brake fluid used for the exposure tests of this study.

* Aftermarket brake fluid used for the exposure tests of this study. The pH of the uninhibited version of the brake fluid was reported to be in the range between 5 and 6.

Table IV

Electrochemical aging conditions and chemistry modification for the uninhibited brake fluid base and the aftermarket brake fluid.

Quantity, units	Uninhibited Brake Fluid Base	Aftermarket Brake Fluid
Volume of Brake Fluid, mL	100	100
Water Added, mL	3	2
1 mol/L NaCl Added, mL	1	1
1 mol/L HCl Added, mL	1	0
Electrode Seperation, mm	30	30
Applied Current, mA	10	10
Current Density, A/m^2	30.7	30.7
Time, s	18480	18000
Charge, coul.	184.8	180.0
Mass Fraction Water, % †	4.59	2.81
Mass Fraction Cu Ions ‡	5.58×10^{-4}	5.54×10^{-4}
Mass Fraction, Cl ions	6.51×10^{-4}	3.31×10^{-4}

† Upper bound which assumes no water loss during charging.
‡ Upper bound which assumes 100% anodic current efficiency, no Cu precipitation from solution, no Cu deposition on cathode, and an ionic charge of 2.

Table V

Brake fluid conductivity measurement results.

Uninhibited Brake Fluid	Measured Resistance (Ω)	Std. Dev. of Meas. (Ω)	Solution Conductivity (μS/m)	Standard Uncertainty (μS/m)
Neat	3.76E+06	1.15E+05	26.54	0.85
2% Water Added	2.52E+06	1.93E+04	39.52	0.48
2% Water and 2% 1 mol/L NaCl	2.53E+04	3.24E+03	3,942	507
Cu Charged	2.90E+04	7.50E+01	3,434	33

Aftermarket Brake Fluid	Measured Resistance (Ω)	Std. Dev. of Meas. (Ω)	Solution Conductivity (μS/m)	Standard Uncertainty (μS/m)
Neat	1.00E+05	2.34E+02	992.9	9.7
2% Water Added	8.11E+04	3.46E+02	1,229	13
2% Water and 2% 1 mol/L NaCl	1.51E+04	1.83E+02	6,581	101
Cu Charged	1.48E+04	8.36E+01	6,724	74

OEM Brake Fluid	Measured Resistance (Ω)	Std. Dev. of Meas. (Ω)	Solution Conductivity (μS/m)	Standard Uncertainty (μS/m)
Neat	1.51E+05	7.67E+03	659.8	34.1
2% Water Added	9.36E+04	1.03E+03	1,065	16
2% Water and 2% 1 mol/L NaCl	2.17E+04	7.97E+01	4,595	47
Thermally Aged	8.20E+04	5.01E+02	1,216	14

Table VI

Open circuit free corrosion measurements for oxygen free grade Cu and pure Fe in the used brake fluid samples supplied by VRTC and the three brake fluid samples used for the exposure tests of this study. Included with this data are the uncertainty for the measurements estimated from the standard deviation of the measurements after steady state was reached and the t-statistic for a test of the significance of the difference between the value measured in the sample compared to the mean for all of the samples.

BF Sample No.	Copper E_{OC}(Cu) (mV)	Meas. Uncertainty (mV)	Significance in t-Test (t value)	Iron E_{OC}(Fe) (mV)	Meas. Uncertainty (mV)	Significance in t-Test (t value)
1	-36.47	0.14	2.25	-9.51	4.48	1.20
2	-53.59	0.55	1.63	12.13	2.75	1.67
3	-47.68	0.51	1.85	45.46	1.93	2.40
4	-73.41	0.92	0.92	-51.53	6.60	0.28
5	-61.02	0.37	1.36	-10.46	6.45	1.17
6	-183.63	0.09	-3.07	-97.17	5.97	-0.72
7	-156.09	0.59	-2.08	-107.93	2.40	-0.95
8	-57.84	4.11	1.48	-21.62	3.12	0.93
9	-148.68	0.18	-1.81	-166.8	1.25	-2.24
10	-77.67	0.29	0.76	-26.9	1.62	0.82
11	-82.35	4.38	0.59	29.35	0.88	2.04
12	-69.61	0.40	1.05	-35.96	0.41	0.62
13	-121.16	0.49	-0.81	-96.42	0.33	-0.70
14	-74.35	0.32	0.88	-21.86	4.24	0.93
15	-119.49	1.26	-0.75	-44.59	2.79	0.43
16	-113.03	0.90	-0.52	-89.8	4.23	-0.56
17	-79.32	0.06	0.70	6.56	3.19	1.55
18	-115.64	0.08	-0.61	-43.88	2.52	0.44
19	-43.37	0.14	2.00	-58.34	2.29	0.13
20	-129.61	0.21	-1.12	-159.63	0.61	-2.08
21*	-102.1	0.16	-0.12	-60.93	1.73	0.07
22†	-110.79	1.16	-0.44	-206.65	3.20	-3.11
23‡	-213.48	1.77	-4.15	-261.4	0.55	-4.30

* Thermally Aged OEM brake fluid used for exposure tests.
† Electrochemically aged uninhibited brake fluid base used for expousre tests (after exposure tests).
‡ Electrochemically aged aftermarket brake fluid with 1 mL of water and 1 mL of 1 mol/L HCl added for exposure tests (after exposure tests).

Table VII

Reciprocal of the charge transfer resistance, which is proportional to the corroson rate, estimated for Cu and Fe in the brake fluids.

Uninhibited Brake Fluid	Cu Corro. Rate (Ω^{-1})	Cu Corro. Rate Error (Ω^{-1})	Fe Corro. Rate (Ω^{-1})	Fe Corro. Rate Error (Ω^{-1})
Neat	1.64 E-05	0.74 E-05	1.15 E-05	0.12 E-05
2% Water Added	1.87 E-05	0.35 E-05	2.16 E-05	0.46 E-05
2% Water and 2% 1 mol/L NaCl	5.14 E-04	0.15 E-04	3.30 E-04	0.18 E-04
Cu Charged	7.26 E-04	0.13 E-04	1.14 E-04	0.05 E-04

Aftermarket Brake Fluid	Cu Corro. Rate (Ω^{-1})	Cu Corro. Rate Error (Ω^{-1})	Fe Corro. Rate (Ω^{-1})	Fe Corro. Rate Error (Ω^{-1})
Neat	1.35 E-05	0.20 E-05	6.75 E-05	0.23 E-05
2% Water Added	1.30 E-05	0.14 E-05	9.57 E-05	0.41 E-05
2% Water and 2% 1 mol/L NaCl	1.90 E-05	0.27 E-05	5.92 E-05	3.77 E-05
Cu Charged	1.31 E-03	0.04 E-03	3.68 E-04	0.33 E-05

OEM Brake Fluid	Cu Corro. Rate (Ω^{-1})	Cu Corro. Rate Error (Ω^{-1})	Fe Corro. Rate (Ω^{-1})	Fe Corro. Rate Error (Ω^{-1})
Neat	1.55 E-05	0.40 E-05	6.76 E-05	0.31 E-05
2% Water Added	2.00 E-05	0.50 E-05	6.62 E-05	0.22 E-05
2% Water and 2% 1 mol/L NaCl	8.01 E-05	0.81 E-05	1.25 E-03	0.46 E-03
Thermally Aged	3.36 E-05	0.28 E-05	5.91 E-05	0.06 E-05

Table VIII

Phases of the copper-water system and their colors.

Phase	**Name**	**Color**
Cu	Copper Metal	Copper Red
Cu_4O	Copper Sub-oxide	Olive Green
Cu_2O	Cuprous Oxide	Red
Cu_2O hydr. or Cu(OH)	Hydrated Cuprous Oxide or Cuprous Hydroxide	Yellow
CuO	Cupric Oxide	Black
CuO hydr. or $Cu(OH)_2$	Hydrated Cupric Oxide or Cupric Hydroxide	Light Blue
Cu_2O_3	Sesquioxide	Reddish Purple
CuO_2	Peroxide	Brown-Black
Cu^{+1}	Cuprous Ion	Colorless
Cu^{+2}	Cupric Ion	Light Blue
$HCuO_2^{-1}$	Bicuprite Ion	Blue
CuO_2^{-1}	Cuprate Ion	Red or Brown

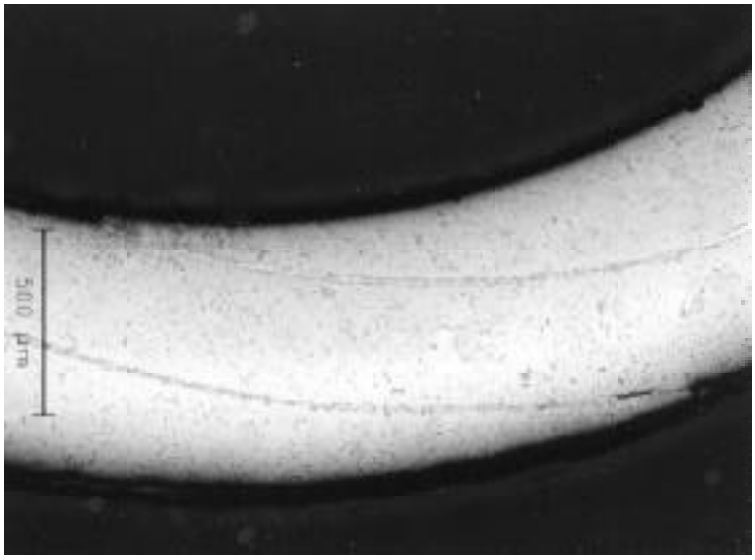

Figure 1

Metallographic cross section through typical brake line showing two layer spiral wrap and copper alloy braze construction (nital etch).

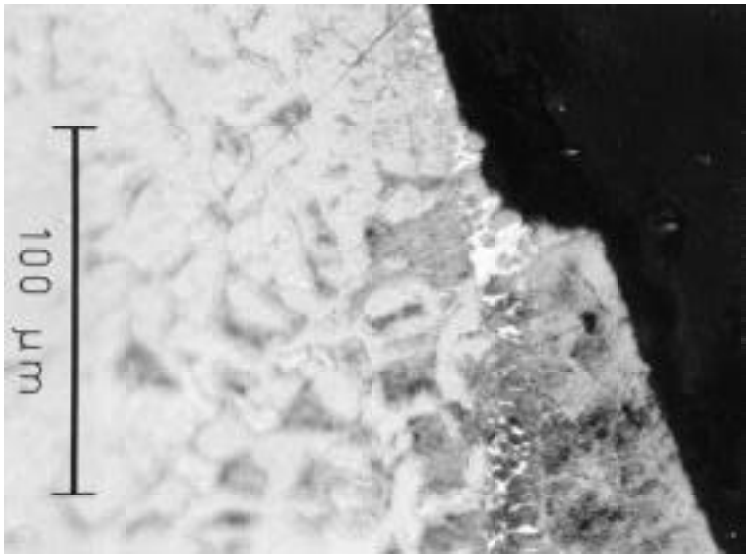

Figure 2

Metallographic cross section through typical brake line showing the the brazed seam at the ID surface with the copper brazing alloy on the ID surface (nital etch).

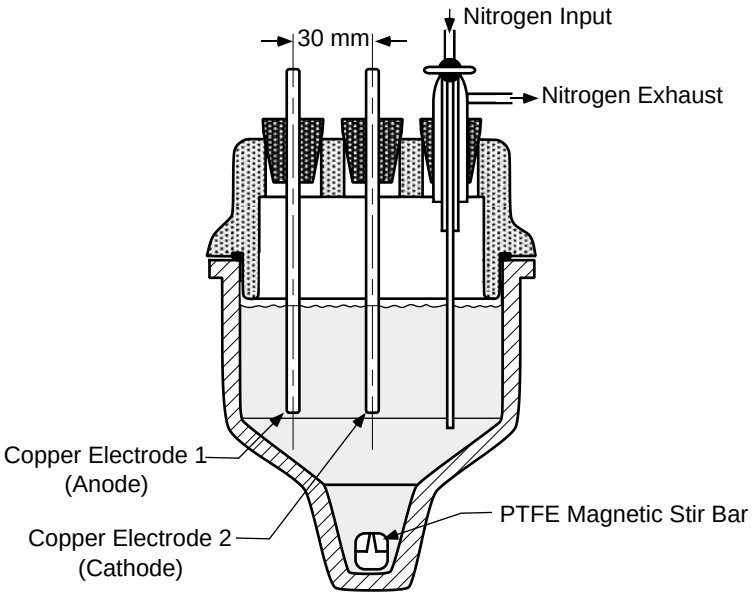

Figure 3

Schematic diagram of the electrochemical cell used to charge brake fluid solutions with copper ions.

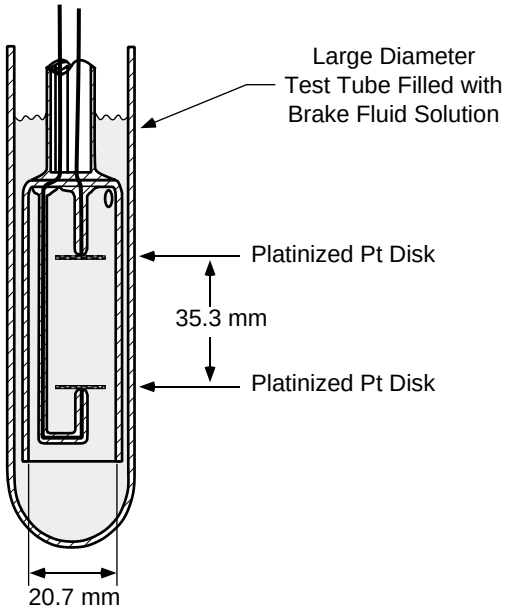

Figure 4

Schematic diagram of the electrolyte conductivity cell used to determine the electrical conductivity of brake fluid solutions.

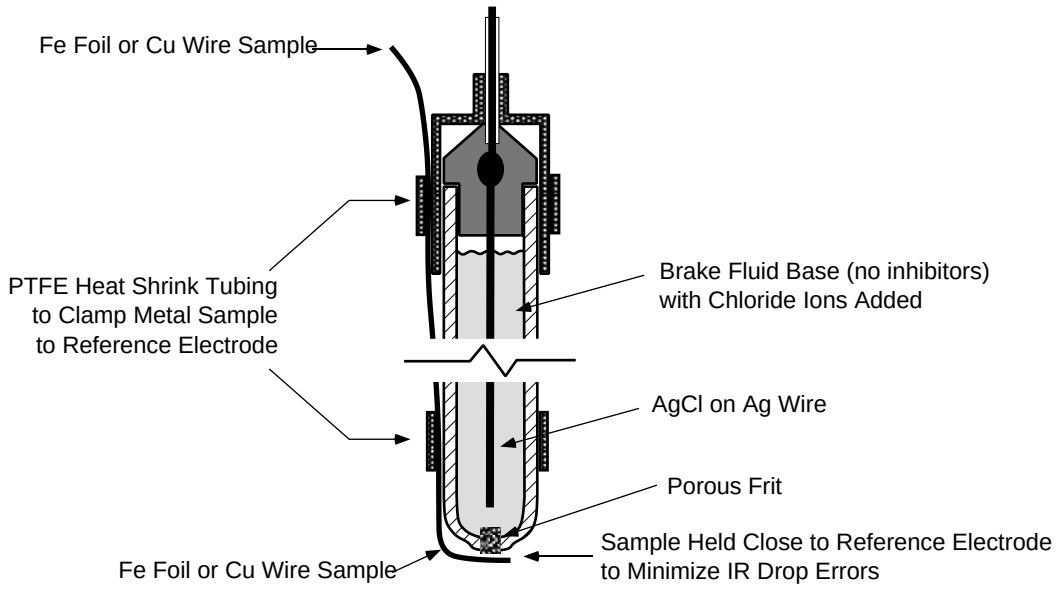

Figure 5

Schematic diagram of the electrode geometry used to measure the open circuit free corrosion potential of pure Fe and oxygen free grade Cu in the brake fluid samples removed from ABS units provided by VTRC.

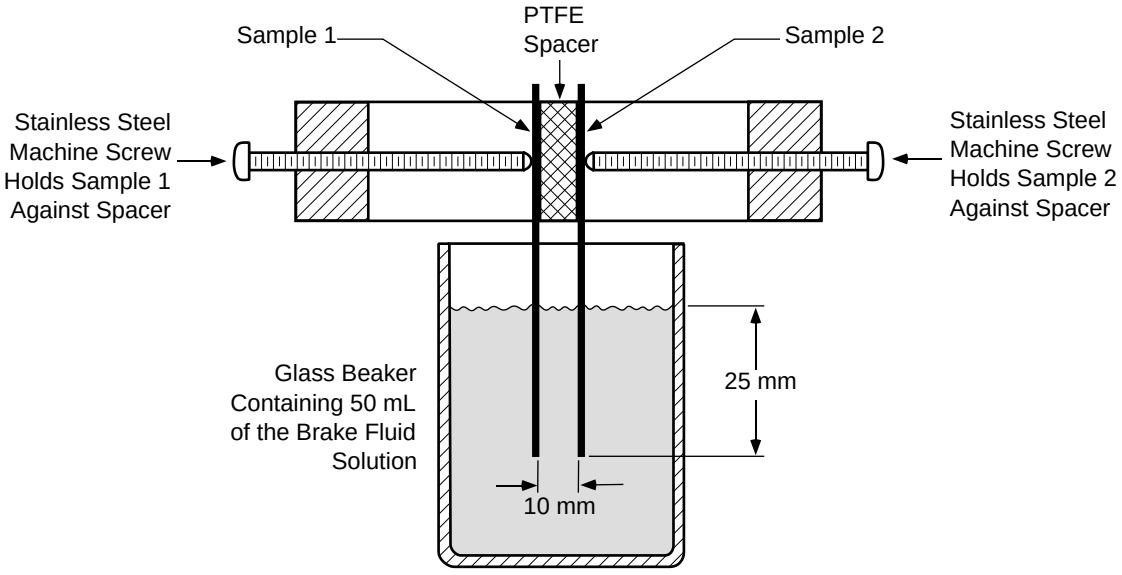

Figure 6

Schematic diagram of the electrode geometry and sample holder used for two electrode ac-impedance measurement of the corrosion rate of oxygen free grade Cu and 1017 steel in brake fluid samples.

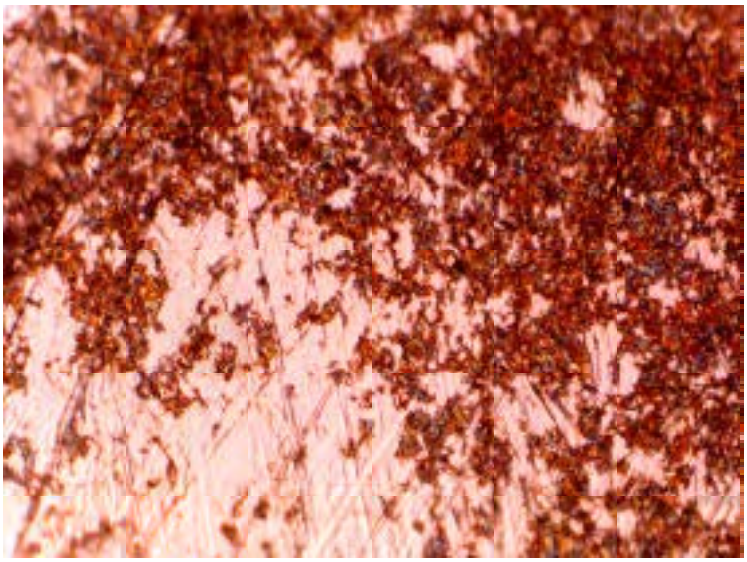

Figure 7

Optical micrograph of the surface of a steel rod after corroding freely in thermally aged OEM brake fluid for 5 hrs.

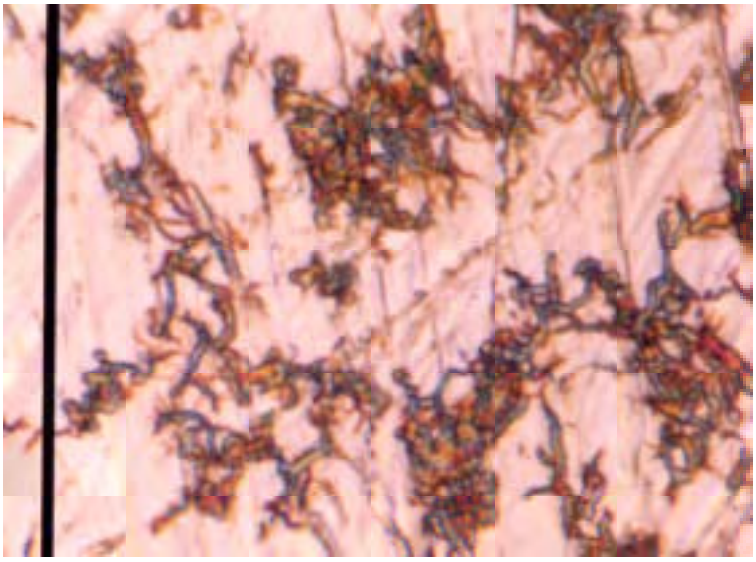

Figure 8

Optical micrograph of the surface of a steel rod after corroding freely in thermally aged OEM brake fluid for 5 hrs.

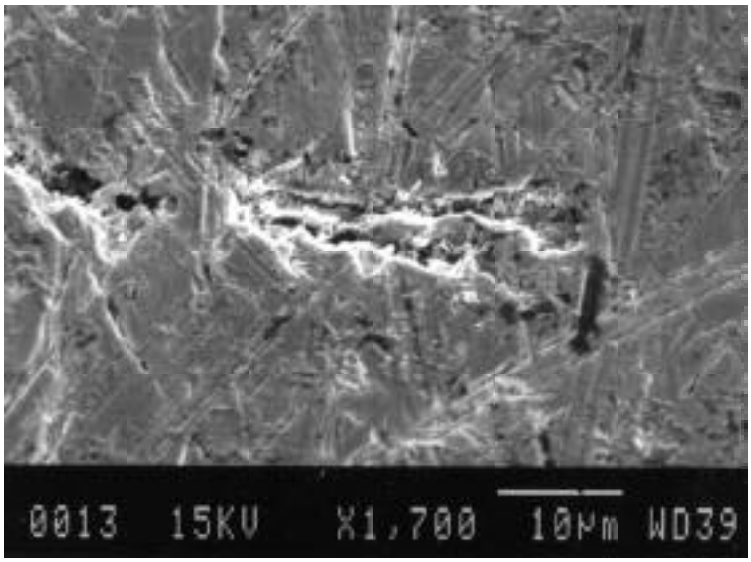

Figure 9

Scanning electron micrograph of the surface of a steel rod after corroding freely in thermally aged OEM brake fluid for 5 hrs.

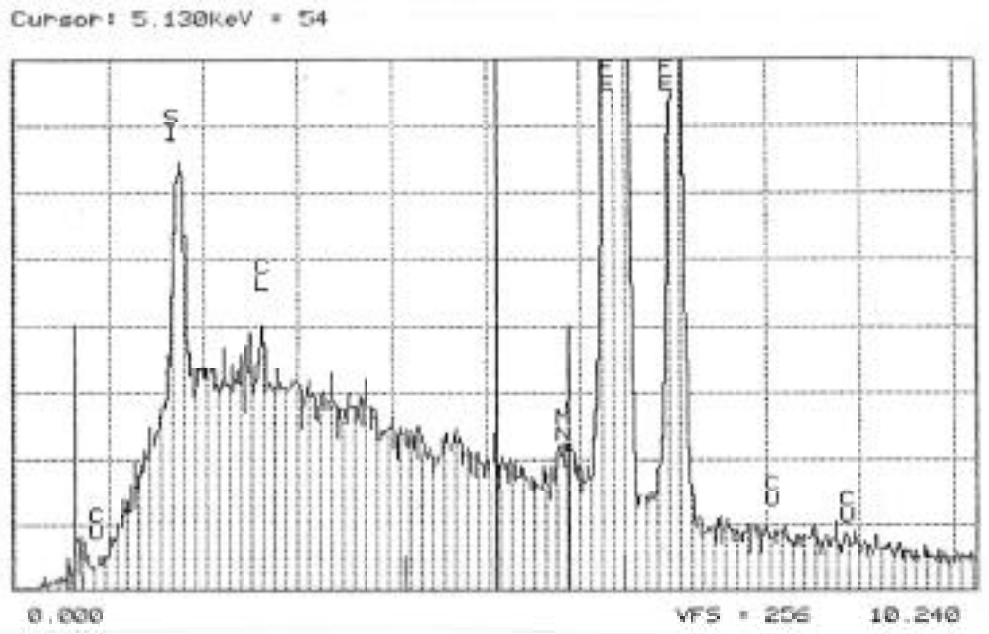

Figure 10

EDS spectrum from surface of a steel rod after corroding freely in thermally aged OEM brake fluid for 5 hrs.

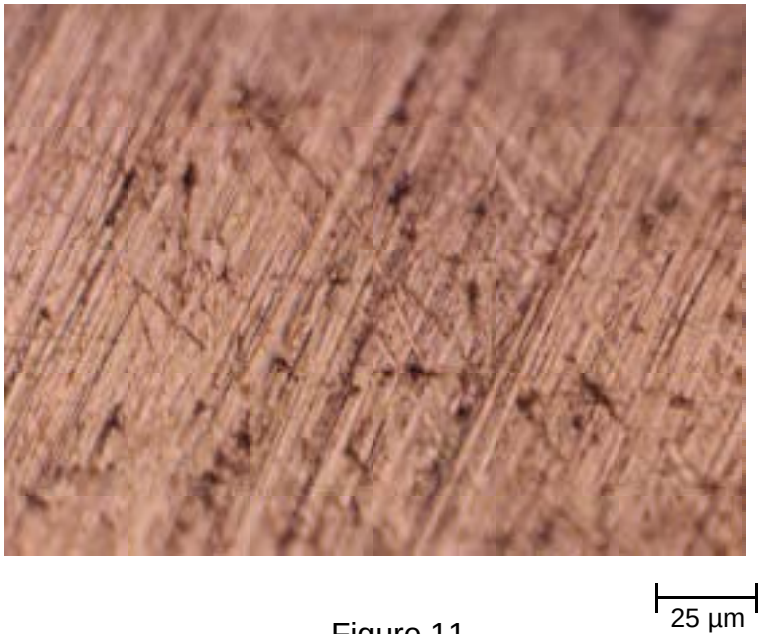

Figure 11

Optical micrograph of the surface of a steel rod after corroding for 13 hours galvanically coupled to a Cu rod of identical size in electrochemically aged aftermarket brake fluid.

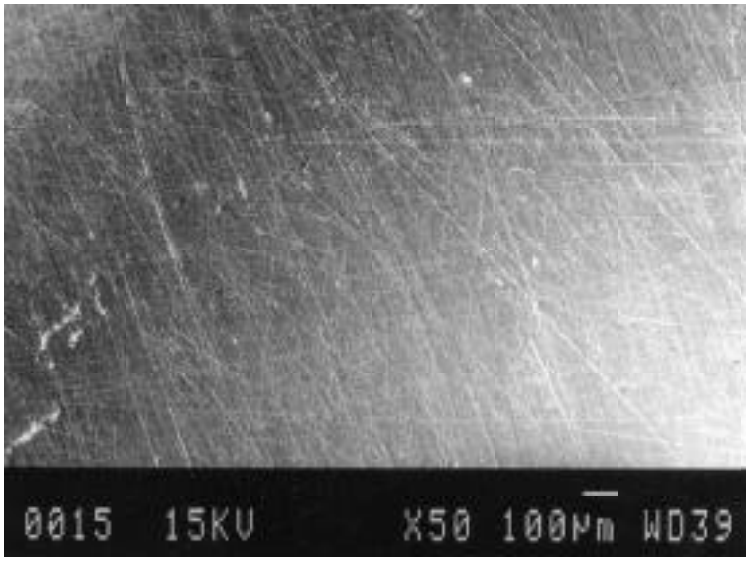

Figure 12

Scanning electron micrograph of the surface of a steel rod after corroding for 13 hours galvanically coupled to a Cu rod of identical size in electrochemically aged aftermarket brake fluid.

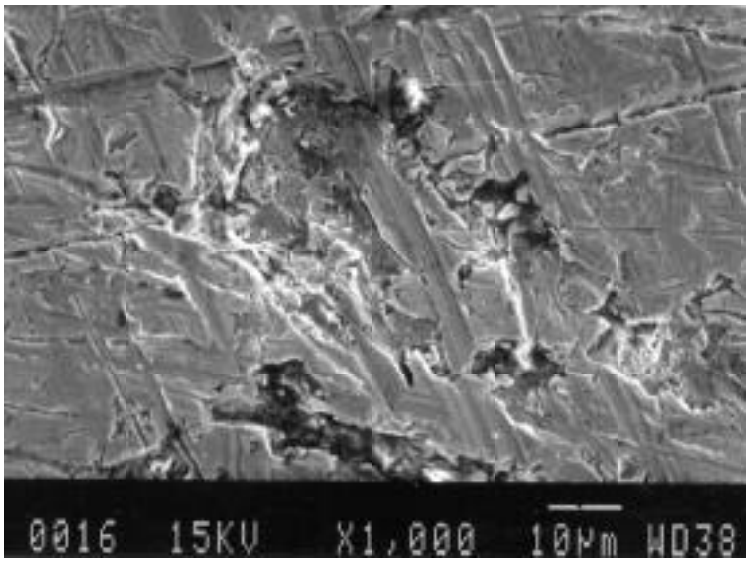

Figure 13

Scanning electron micrograph of the surface of a steel rod after corroding for 13 hours galvanically coupled to a Cu rod of identical size in electrochemically aged aftermarket brake fluid.

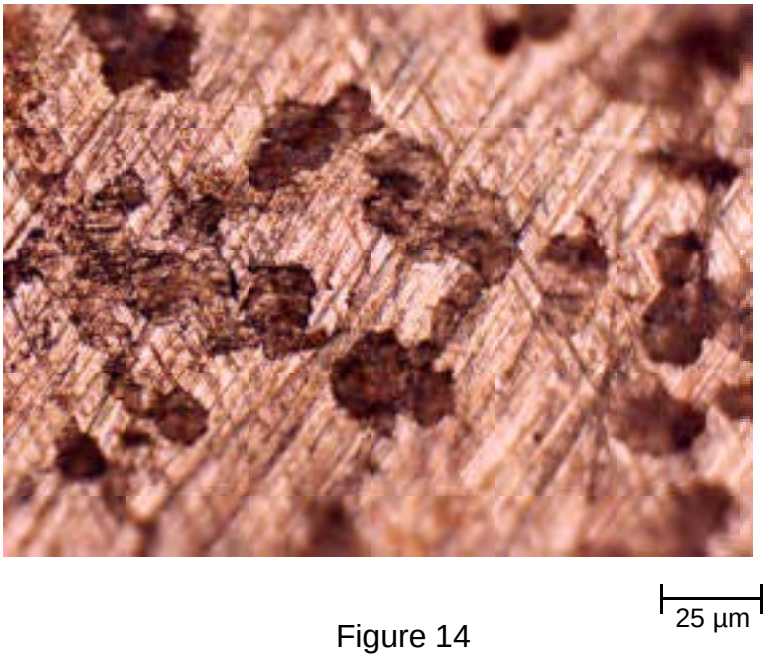

Figure 14

Optical micrograph of the surface of a steel rod after corroding for 5 hours in electrochemically aged aftermarket brake fluid to which 1 mL of water and 1 mL of 1 mol/L HCl had been added.

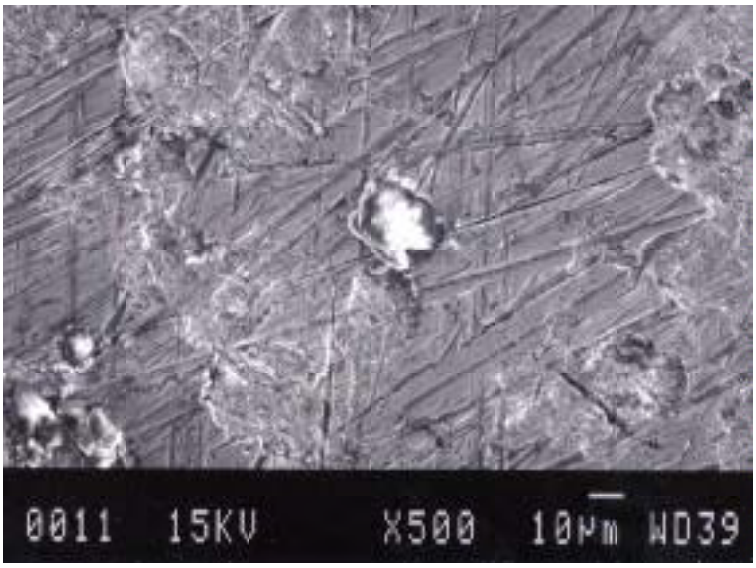

Figure 15

Scanning electron micrograph of the surface of a steel rod after corroding for 5 hours in electrochemically aged aftermarket brake fluid to which 1 mL of water and 1 mL of 1 mol/L HCl had been added.

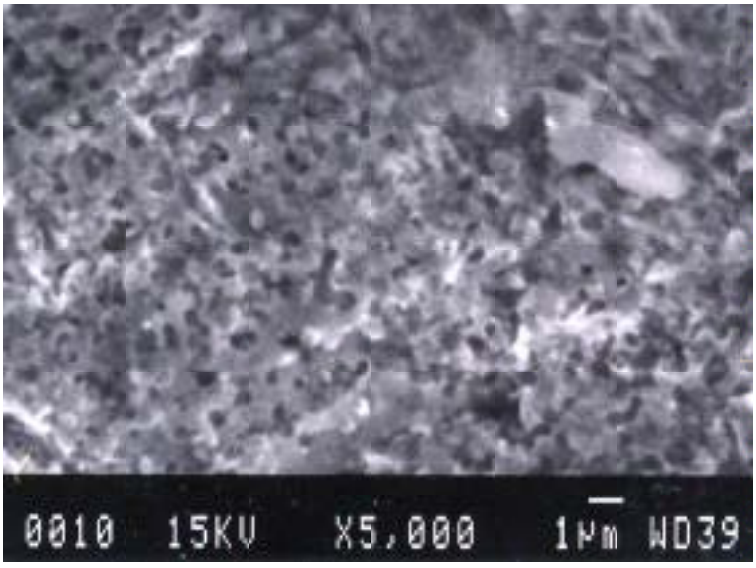

Figure 16

Scanning electron micrograph of the surface of a steel rod after corroding for 5 hours in electrochemically aged aftermarket brake fluid to which 1 mL of water and 1 mL of 1 mol/L HCl had been added.

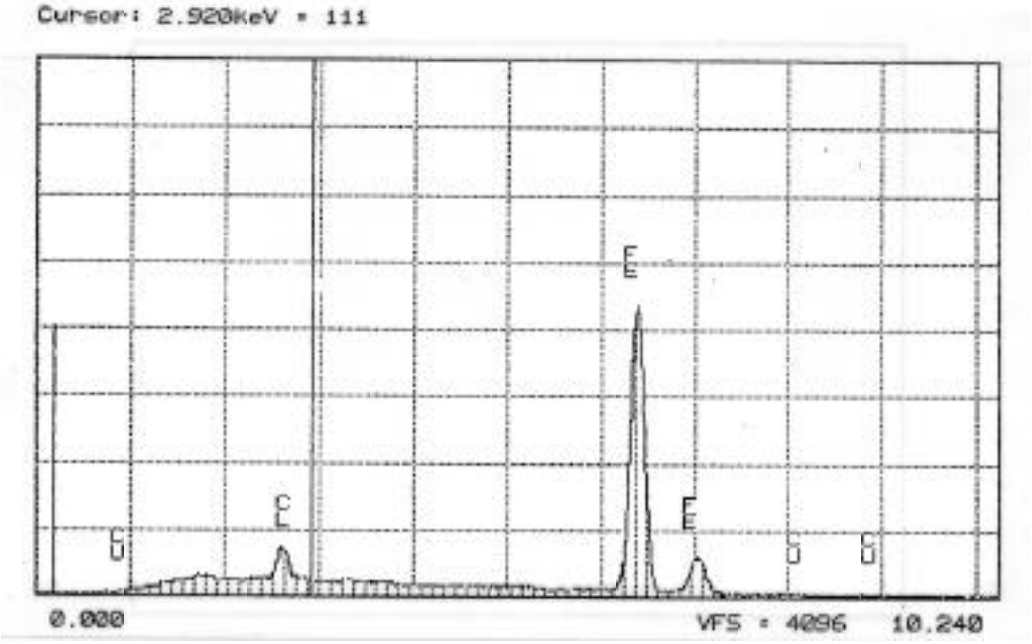

Figure 17

EDS spectrum from the whitish corrosion deposit shown in figure 15.
No evidence of Cu can be seen in this spectrum.

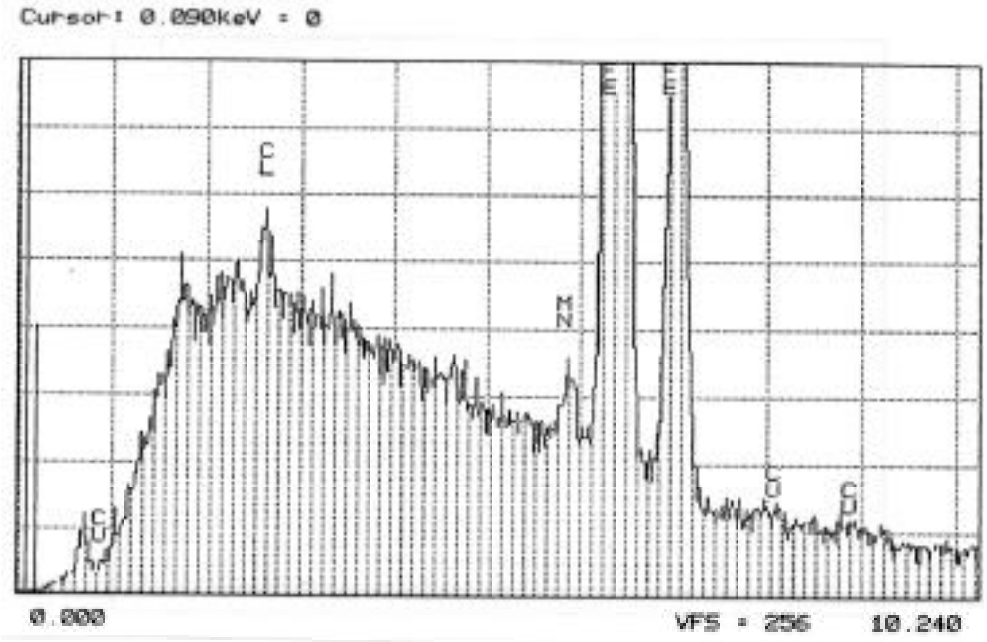

Figure 18

EDS spectrum from the bottom of the shallow pit shown in figure 16.
Small peaks indicating the presence of Cu can be seen in this spectrum.

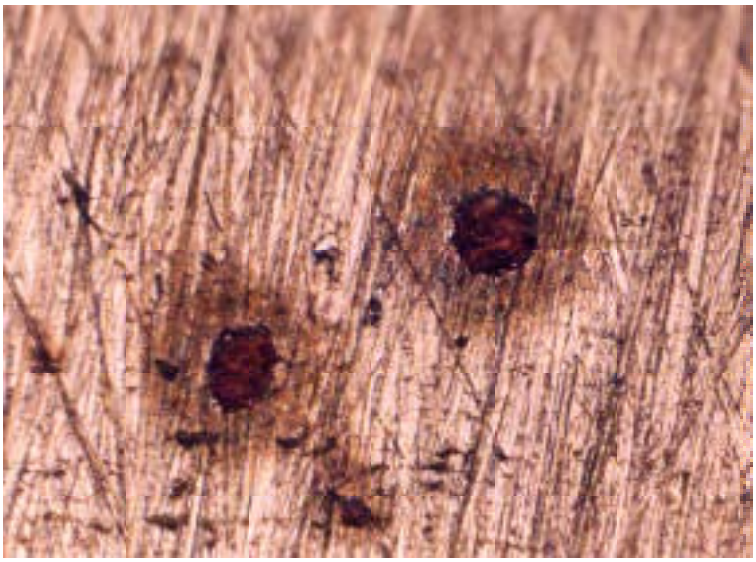

Figure 19

Optical micrograph of the surface of a steel rod after corroding for 5 hours in electrochemically aged uninhibited brake fluid.

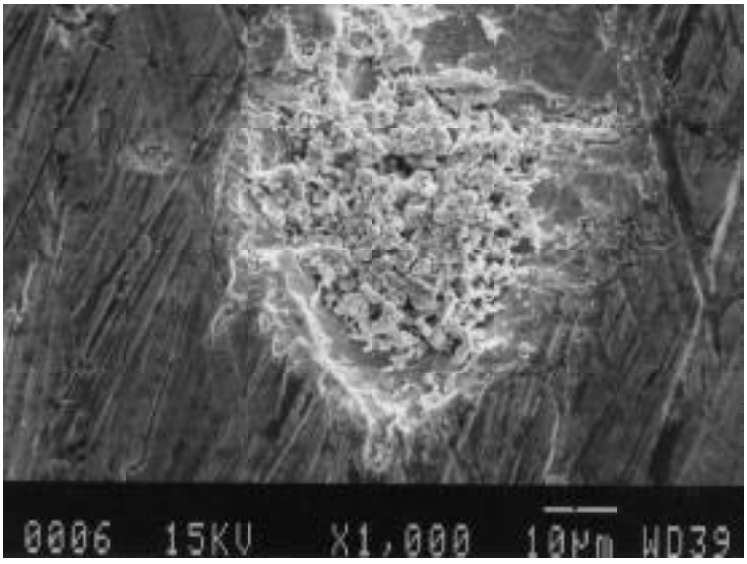

Figure 20

Scanning electron micrograph of a corrosion pit found in the surface of a steel rod after corroding for 5 hours in electrochemically aged uninhibited brake fluid.

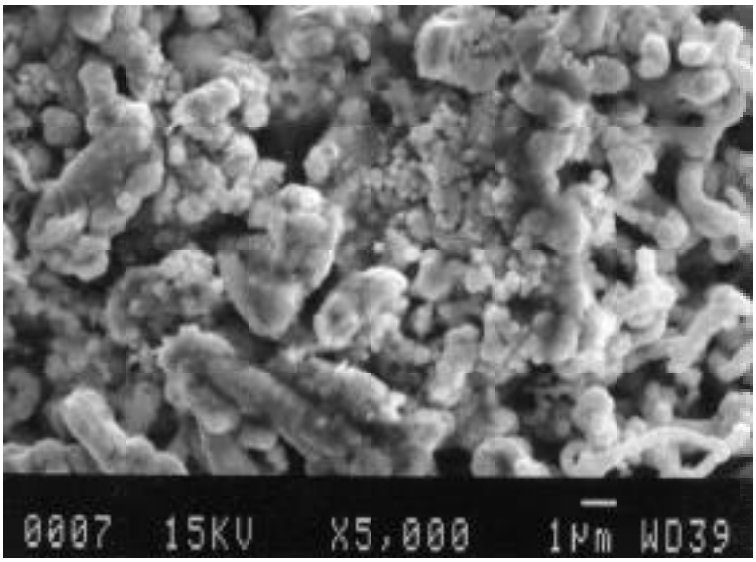

Figure 21

Scanning electron micrograph of the deposits found in a corrosion pit in the surface of a steel rod after corroding for 5 hours in electrochemically aged uninhibited brake fluid.

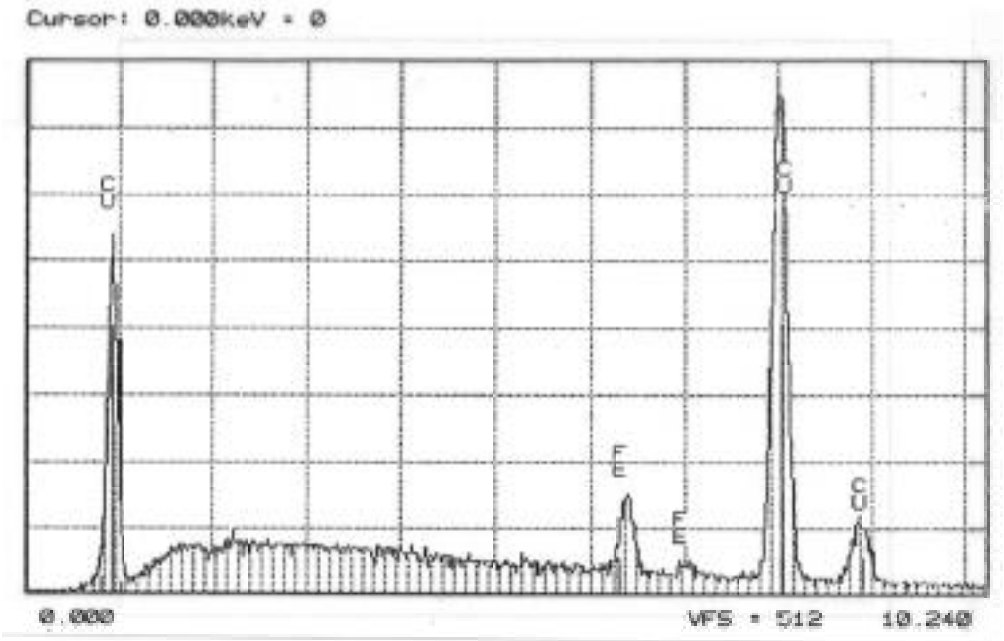

Figure 22

EDS spectrum taken from the deposits inside a corrosion pit in the surface of a steel rod which corroded for 5 hours in electrochemically aged uninhibited brake fluid.

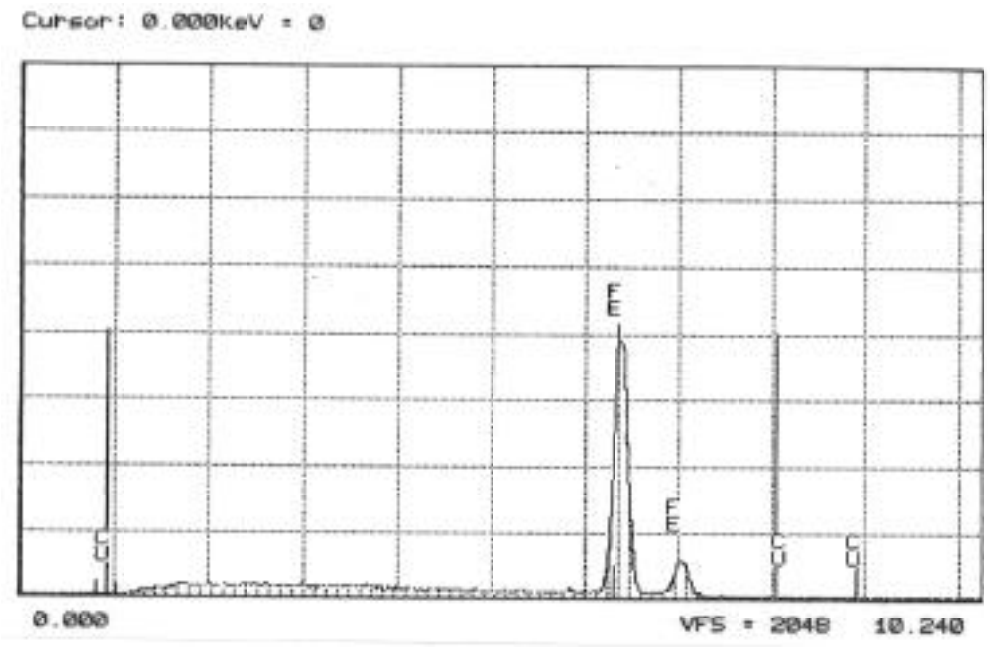

Figure 23

EDS spectrum from an unattacked area of the surface of the steel rod corroded in electrochemically aged uninhibited brake fluid for 5 hrs.

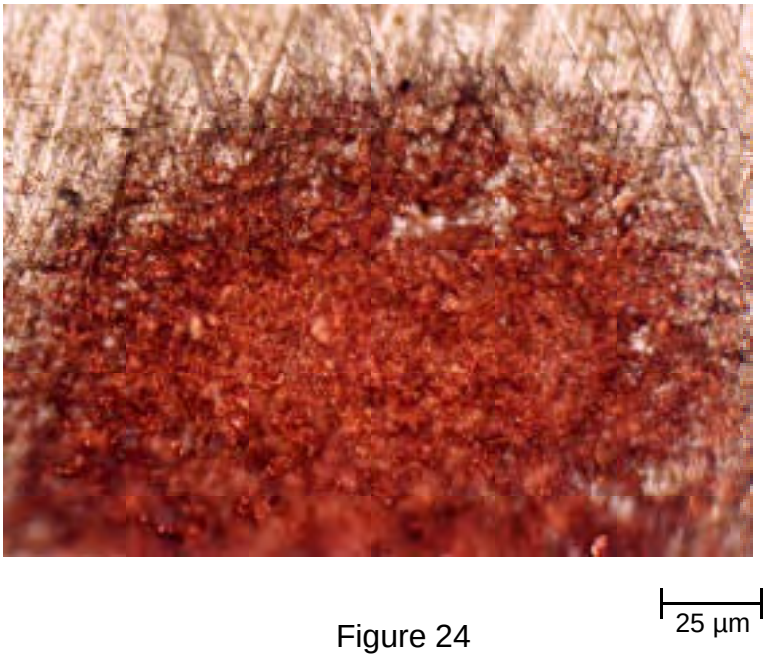

Figure 24

Optical micrograph of the surface of a steel rod after corroding for 14 hours galvanically coupled to a Cu rod of equal size in electrochemically aged uninhibited brake fluid.

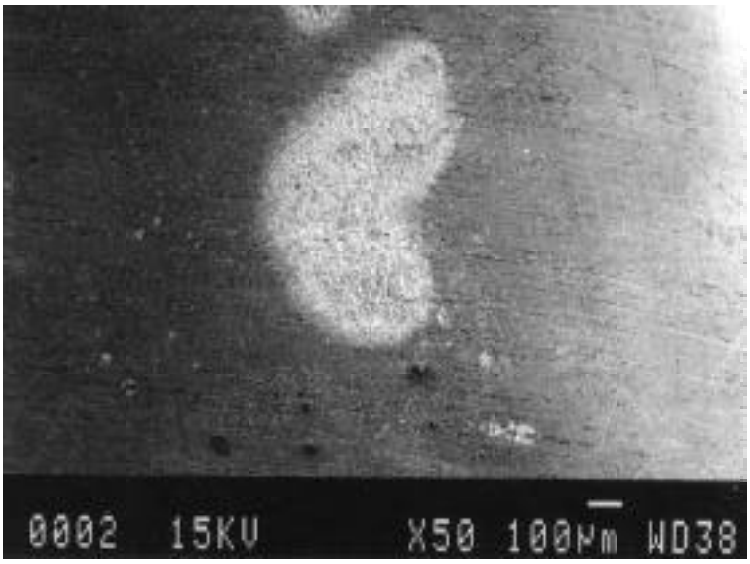

Figure 25

Scanning electron micrograph showing the pits or corrosion patches found in the surface of a steel rod after corroding for 14 hours galvanically coupled to a Cu rod of equal size in electrochemically aged uninhibited brake fluid.

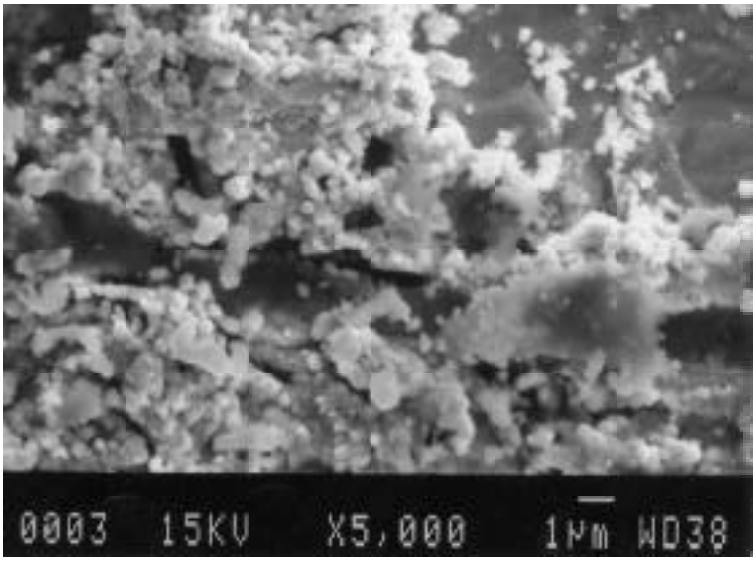

Figure 26

Scanning electron micrograph of the deposits found in the pits or corrosion patches in the surface of a steel rod after corroding for 14 hours galvanically coupled to a Cu rod of equal size in electrochemically aged uninhibited brake fluid.

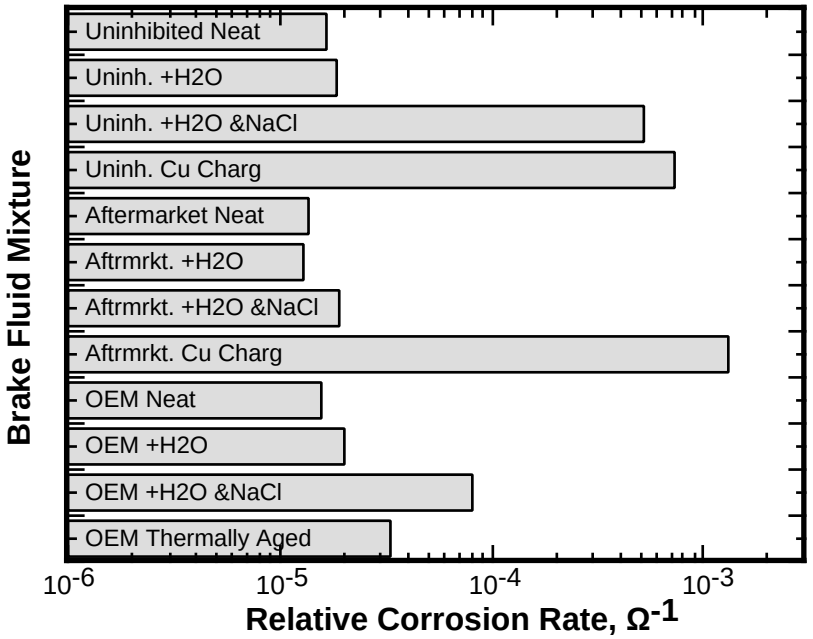

Figure 27

Relative corrosion rates as indicated by the reciprocal of the charge transfer resistance measured during 2 electrode ac-impedance measurments on oxygen free grade copper in different brake fluid mixtures.

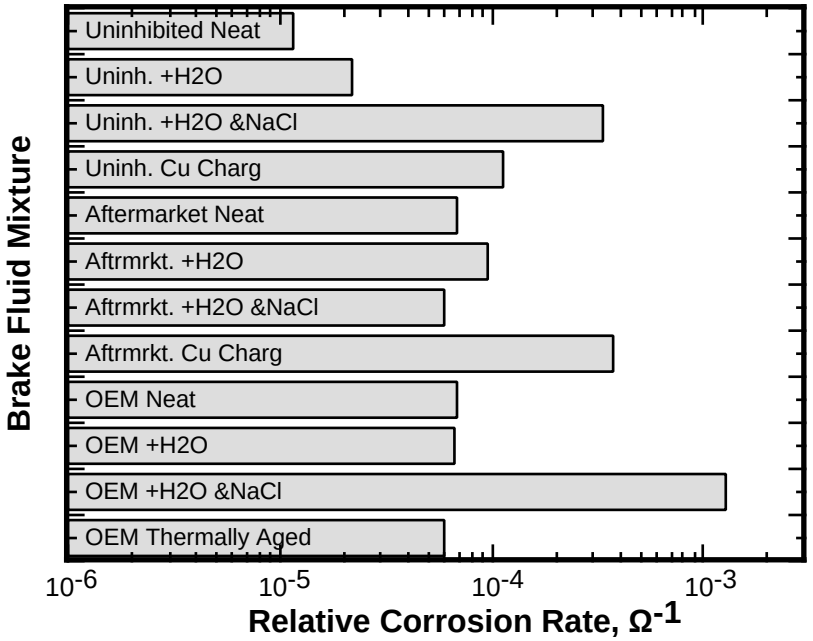

Figure 28

Relative corrosion rates as indicated by the reciprocal of the charge transfer resistance measured during 2 electrode ac-impedance measurments on pure iron in different brake fluid mixtures.

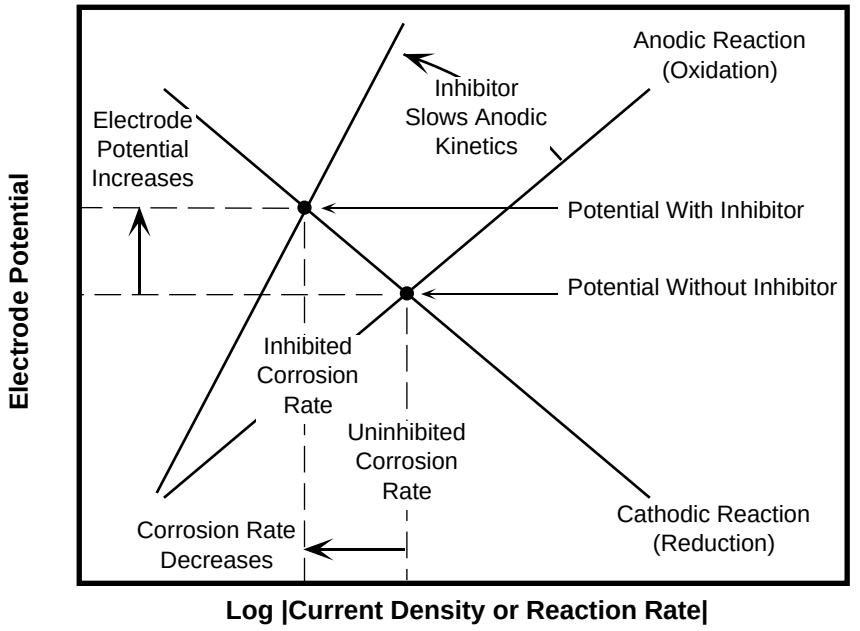

Figure 29(a)

Schematic diagram illustrating the influence of an inhibitor that retards anodic reaction kinetics on the steady state free corrosion potential of an electrode.

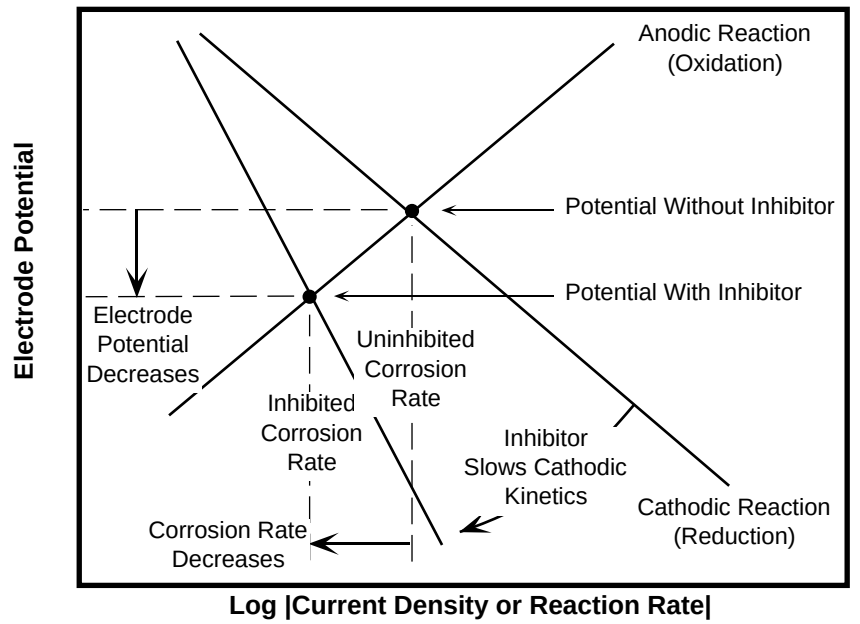

Figure 29(b)

Schematic diagram illustrating the influence of an inhibitor that retards cathodic reaction kinetics on the steady state free corrosion potential of an electrode.

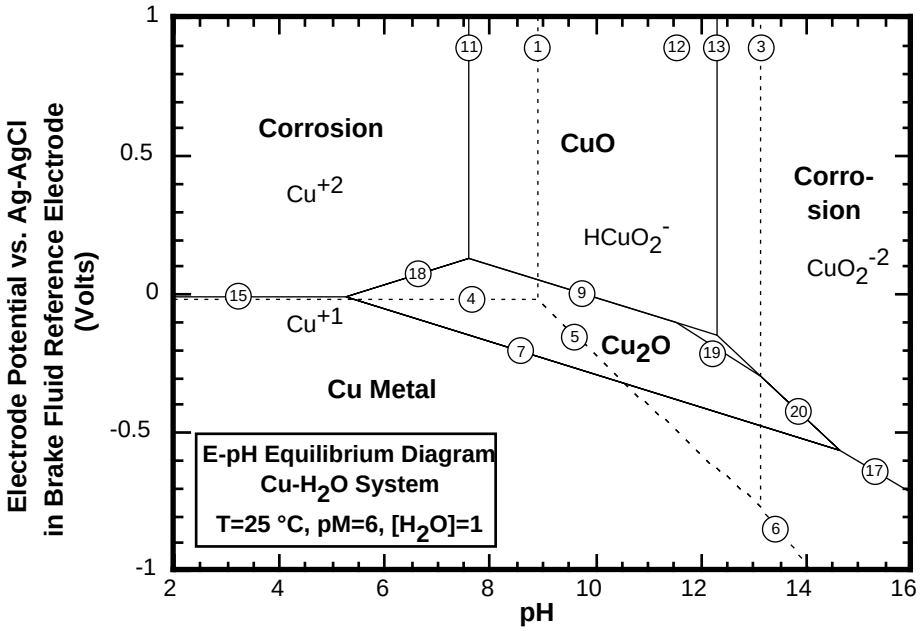

Figure 30

Electrochemical equilibrium (E-pH) diagram for copper-water system with the potential scale converted to the Ag-AgCl in brake fluid reference to enable comparison to measurements in this work (E=0.167 V vs. SHE).

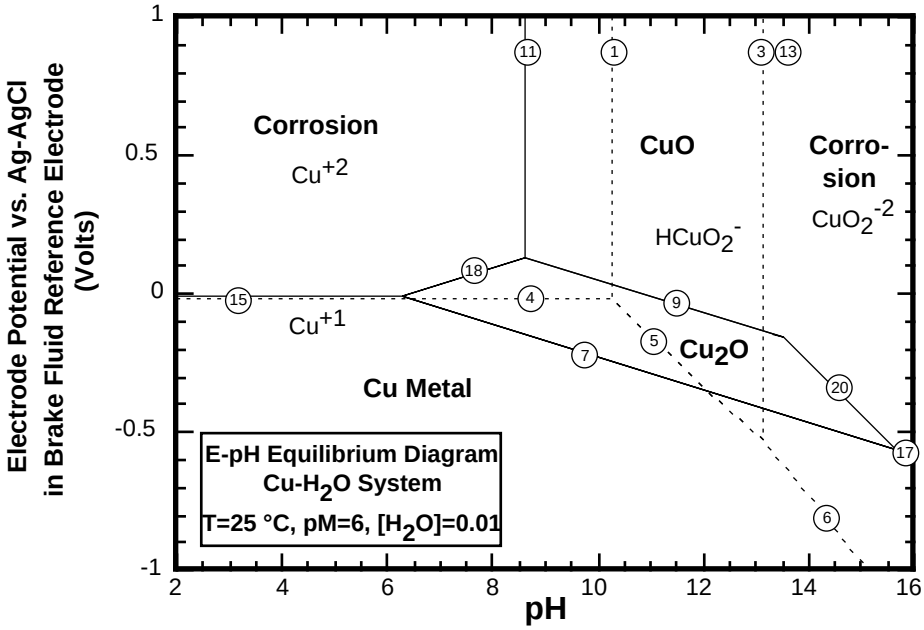

Figure 31

Electrochemical equilibrium diagram for copper-water system as in figure 28 above, but with the activity of water set at 0.01 (1%) to represent equilibria in water contaminated brake fluid.

Appendix A

Materials Safety Data Sheet for Delco Supreme 11 Brake Fluid

GENERAL MOTORS CORPORATION
MATERIAL SAFETY DATA SHEET

==========
(P) DELCO SUPREME II BRAKE FLUID
1052542
5464833
5464832
5464834
5464830
11G
11Q
11-5
11-12
* 1052535

SECTION 0 -- EFFECTIVE DATE

1 -->Effective Date: 042178
2 -->MSDS signed by: Not Provided
3 -->Title: Not Provided

SECTION 1 -- SHIPPING INFORMATION

1 -->Chemical Family: POLYALKYLENE GLYCOL AND GLYCOL ETHERS
2 -->Formula: Not Provided

(*)MID: #536166
DELCO MORAINE DIV GMC
DUNS Account #: 00-425-5352
Emergency telephone #: 513/455-6240
1420 WISCONSIN BLVD
DAYTON, OH 45401

Shipping Name:
Hazard Class:
U.N. Code:
Flash Point: 265 F COC

SECTION 2 -- INGREDIENTS

CAS#	Formulation	Chemical Name
989916176	20 /30% BY WT	POLYALKYLENE GLYCOL LUBRICANT
989902339	62 /79% BY WT	GLYCOL ETHERS
989923001	= 2% BY WT	INHIBITORS
989953019	1 /6% BY WT	REACTED CASTOR OIL - MIXED POLYPROPYLENE GLYCOL LUBRICANT

SECTION 3 -- PHYSICAL DATA

1 -->Boiling Point: 450F
2 -->Specific Gravity: 1.026
3 -->Vapor Pressure: <0.1 MM HG @ 20C
4 -->% Volatile by Volume: NIL
5 -->% Solid by Weight: Not Provided
6 -->Vapor Density: >1
7 -->Evaporation Rate: <0.01 (BUAC=1)
8 -->Solubility in H2O: MISCIBLE
9 -->pH: 10.3
10 -->Appearance & Odor: CLEAR LIQUID / MILD GLYCOL ETHER
11 -->State: LIQUID

SECTION 4 -- FIRE AND EXPLOSION DATA

1 -->Flammable Limits - LEL: Not Provided
2 -->Flammable Limits - UEL: Not Provided
3 -->Extinguishing Media: WATER, CO2, DRY CHEMICAL
4 -->Special Fire Fighting Procedures: NONE
5 -->Unusual Fire & Explosion Hazards: NONE

SECTION 5 -- HEALTH HAZARD DATA

1 -->Effects of Overexposure: CONTINUAL CONTACT SLIGHTLY IRRITATING TO SKIN ON SOME PEOPLE.
2 -->Threshold Limit Value: NOT APPLICABLE
3 -->Permissible Exposure Limit: Not Provided
4 -->Other Limit: Not Provided
5 -->Primary routes of entry: Not Provided
6 -->Emergency First Aid Procedures: SKIN AND EYES: FLUSH WITH COPIOUS AMOUNTS OF WATER. INGESTION: CONTACT PHYSICIAN IMMEDIATELY.

SECTION 6 -- REACTIVITY DATA

1 -->Stable: YES
2 -->Conditions to Avoid: NONE
3 -->Incompatible Materials: NONE
4 -->Hazardous Decomposition Products: THERMAL DECOMPOSITION OR BURNING MAY PRODUCE CARBON MONOXIDE AND/OR CARBON DIOXIDE AND TRACE QUANTITIES OF NITROGEN OXIDES.
5 -->Can Hazardous Polymerization Occur: NO
6 -->Conditions to Avoid: NONE

SECTION 7 -- SPILL OR LEAK PROCEDURES

1 -->Steps to be taken in case material is released or spilled: COLLECT SPILLAGE WITH ABSORPTIVE MEDIA.
2 -->Waste Disposal Method: INCINERATE IN AN APPROVED FACILITY.
3 -->CERCLA (Superfund) Reportable quantity (lbs): Not Provided
4 -->RCRA Hazardous Waste No. (40 CFR 261.33): Not Provided
5 -->Volatile Organic Compound (VOC) Theoretical: Not Provided
6 -->Volatile Organic Compound (VOC) Analytical: Not Provided

SECTION 8 -- SPECIAL PROTECTION INFORMATION

1 -->Respiratory Protection: NOT NEEDED
2 -->Local Exhaust: Not Provided
3 -->Special: Not Provided
4 -->Mechanical: ACCEPTABLE
5 -->Other: Not Provided
6 -->Protective Gloves (Specify type): RUBBER GLOVES RECOMMENDED
7 -->Eye Protection (Specify type): SAFETY GLASSES RECOMMENDED
8 -->Other Protective Equipment: NONE

SECTION 9 -- SPECIAL PRECAUTIONS

1 -->Precautions to be taken in Handling & Storage: STORE IN A DRY PLACE AT AMBIENT TEMPERATURE.
2 -->Other Precautions: NONE

SECTION 10 -- ADDITIONAL DATA

1 -->Additional Health Hazard Data: Not Provided

==========

Appendix B

Materials Safety Data Sheet for Emkadixol 310 Brake Fluid

UNION CARBIDE CORPORATION
MATERIAL SAFETY DATA SHEET

EFFECTIVE DATE 03/30/98

Union Carbide urges each customer or recipient of this MSDS to study it carefully to become aware of and understand the hazards associated with the product. The reader should consider consulting reference works or individuals who are experts in ventilation, toxicology, and fire prevention, as necessary or appropriate to use and understand the data contained in this MSDS.

To promote safe handling, each customer or recipient should: (1) notify its employees, agents, contractors and others whom it knows or believes will use this material or the information in this MSDS and any other information regarding hazards or safety; (2) furnish this same information to each of its customers for the product; and (3) request its customers to notify their employees, customers, and other users of the product of this information.

I. IDENTIFICATION

PRODUCT NAME:	EMKADIXOL 310 Brake Fluid
CHEMICAL NAME:	Not applicable (mixture)
CHEMICAL FAMILY:	Glycol ethers
FORMULA:	Inhibited mixture of Polyalkylene glycols & glycol ethers.
MOLECULAR WEIGHT:	Not applicable (mixture)
SYNONYMS:	None
CAS # AND NAME:	See Section III, "Ingredients"

II. PHYSICAL DATA

BOILING POINT, 760 mm Hg:	259.6 C (499.3 F)
SPECIFIC GRAVITY(H2O = 1):	1.039 at 20/20 C
FREEZING POINT:	Pour point -51 C (-60 F)
VAPOR PRESSURE AT 20°C:	<0.01 mmHg

EMERGENCY PHONE NUMBERS: 1-800-UCC-HELP (NUMBER AVAILABLE AT ALL TIMES) OR (304) 744-3487

UNION CARBIDE CORPORATION
39 Old Ridgebury Road, Danbury, CT 06817-0001

VAPOR DENSITY (AIR = 1): 6

EVAPORATION RATE (Butyl Acetate = 1): <0.01

SOLUBILITY IN WATER by wt: With haze
100% at 20 C

APPEARANCE: Transperent yellow

ODOR: Mild

PHYSICAL STATE: Liquid

PERCENT VOLATILES (by weight): 2.8

III. INGREDIENTS

%	MATERIAL	CAS#	EXPOSURE LIMIT
0-50	Triethylene glycol monoethyl ether	112-50-5	None established
0-40	Triethylene Glycol Monomethyl Ether	112-35-6	None established
0-35	Triethylene Glycol Monobutyl Ether	143-22-6	None established
5-30	Polyethylene Glycol	25322-68-3	None established
0-25	Polyethylene glycol monobutyl ether	9004-77-7	None established
0-25	Polyethylene glycol monomethyl ether	9004-74-4	None established
0-10	Triethylene Glycol	112-27-6	See Section V
0-10	Diethylene glycol monobutyl ether	112-34-5	None established
0-5	Diethylene Glycol	111-46-6	See Section V
0-4	Diethylene Glycol Monomethyl Ether	111-77-3	None established
0-3	Diethylene glycol monopropyl ether	6881-94-3	None established
0-2	Trade secret inhibitor package	None	None established

IV. FIRE AND EXPLOSION HAZARD DATA

FLASH POINT:

280 F (137.7 C)
Pensky-Martens Closed Cup ASTM D 93

335 F (168.3 C)
Cleveland Open Cup ASTM D 92

FLAMMABLE LIMITS IN AIR % by volume: LOWER: Not Determined UPPER: Not Determined

EXTINGUISHING MEDIA: Apply alcohol-type or all-purpose-type foam by manufacturers' recommended techniques for large fires. Use water spray, carbon dioxide, or dry chemical media for small fires.

SPECIAL FIRE FIGHTING PROCEDURES: Do not direct a solid stream of water or foam into hot, burning pools; this may cause frothing and increase fire intensity.
Use protective clothing, eye protection and have self-contained breathing apparatus available.

UNUSUAL FIRE AND EXPLOSION HAZARDS: During a fire, oxides of nitrogen may be produced.
See "Other Precautions" in Section IX.

V. HEALTH HAZARD DATA

EXPOSURE LIMIT(S): Diethylene Glycol: AIHA WEEL
50 ppm TWA 8hr. vapor and aerosol
10 mg/m3 TWA 8hr. aerosol
Triethylene Glycol: 100 mg/m3 TWA, Internal Exposure Limit

EFFECTS OF ACUTE OVEREXPOSURE:

SWALLOWING: Slightly toxic. May cause abdominal discomfort, nausea, and vomiting.

SKIN ABSORPTION: Prolonged or widespread contact may result in the absorption of potentially harmful amounts of material.

INHALATION: Short-term harmful health effects are not expected from vapor generated at ambient temperature.

SKIN CONTACT: Prolonged or repeated contact may cause discomfort and local redness.
Prolonged or repeated contact may cause defatting and drying of the skin.

EYE CONTACT: Causes severe irritation, experienced as discomfort or pain, excess blinking and tear production, with marked excess redness and swelling of the conjunctiva.

EFFECTS OF REPEATED OVEREXPOSURE:
Exposure to high concentrations of aerosol generated at room temperature may

cause lung injury and liver dysfunction.

OTHER HEALTH HAZARDS:

Skin contact may cause sensitization and an allergic skin reaction.
Components of this formulation have caused slight embryofetal toxicity (delayed development), but no increase in birth defects in laboratory animals.

MEDICAL CONDITIONS AGGRAVATED BY OVEREXPOSURE:

Skin contact may aggravate an existing dermatitis.

ADDITIONAL TOXICITY INFORMATION:

Evidence of kidney and liver injury was observed in rats receiving triethylene glycol monoethyl ether at concentrations of 0.5% and greater in drinking water for 30 days.
In studies in rats, triethylene glycol monomethyl ether produced testicular atrophy when administered in drinking water over a 90-day period at a dosage level of 4 g/kg/day. This effect was not seen at oral dosage levels of 1.2 g/kg/day or when applied to the skin for 90 days at the highest dosage level attainable, 4 g/kg/day.
Evidence of developmental toxicity in the presence of maternal toxicity was noted in offspring of pregnant rats receiving large oral doses of triethylene glycol monomethyl ether. Doses of 1250 mg/kg/day and higher, administered during the period of organogenesis, were associated with effects typically attributed to delayed development. A dose of 1000 mg/kg was a clear No Observed Effects Level (NOEL) for developmental toxicity in this species. No evidence of developmental toxicity was noted in rabbits even at doses as high as 1500 mg/kg, a dose which was severely toxic to the mothers.
Contains one or more amines which may react with nitrites to form nitrosamines. Some nitrosamines have been shown to be carcinogenic in laboratory animals.
Triethylene glycol was given to rats by inclusion in the diet for 90 days at concentrations of 10,000, 20,000 or 50,000 ppm. At the highest dose, there were decreases in body weight. Physiologic responses to these high doses were observed in kidney weight and urinalysis. No specific organ toxicity was seen.
In a 9-day (whole body) repeated inhalation exposure (6 hr/day) study with rats, mortality occurred at 4284 mg/m3 effects included eye irritation and increased alanine aminotransferase and alkaline phosphatase activities; at 494 mg/m3 there was slightly increased alkaline phosphatase activity.
In a subsequent 9-day (nose-only) repeated aerosol study rats were exposed to concentrations up to 1036 mg/m3. The only effect noted was slight (not statistically or biologically significant) decrease in body weight gain at 51 and 1036 mg/m3, but not at 102 mg/m3. No indications of local or systemic target organ toxicity were noted, including effects on hematology, clinical chemistry or urinalysis.
In a sensory irritation study in mice, exposure to high concentrations of triethylene glycol aerosol resulted in a decreased respiratory rate. The RD50, or concentration which produced a 50% decrease in respiratory rate, was 5.1 mg/l.
There was no evidence in developmental toxicity studies for either embryotoxic or teratogenic effects in mice or rats given triethylene glycol by gavage. Maternal toxicity was seen as reduced body weight and food consumption, increased water consumption, and increased relative kidney weight with rats, and clinical signs and increased relative kidney weight with mice.
There was no histologic evidence of damage to the kidneys in either species. The no-observable effect doses for maternal toxicity were 1125 mg/kg/day for rats and 5630 mg/kg/day for mice. Minor fetotoxicity (reduced fetal body weights and increased skeletal variations) was present with doses of 11260 mg/kg/day for rats, and 5630 and 11260 mg/kd/day for mice. The no-observable effect dose for fetotoxicity was 5630 mg/kg/day for rats and 563 mg/kg/day for mice.
A chronic dietary feeding study of diethylene glycol with rats showed mild kidney injury at 1%, while concentrations of 2% and 4% caused more marked kidney injury. In addition, at 2% and 4% of diethylene glycol in the diet,

some rats developed benign papillary tumors in the urinary bladder. These have been attributed to the presence of urinary bladder calcium oxalate stones. No evidence for carcinogenicity was found with a chronic skin-painting study with diethylene glycol in mice. The absence of a direct chemical carcinogenic effect accords with the results in in vitro genotoxicity studies which show that it does not produce mutagenic or clastogenic effects. A feeding study employing up to 5.0% diethylene glycol in the diet failed to produce any teratogenic effects.
In a mouse continuous breeding study with large doses of diethylene glycol in drinking water, there was evidence for reproductive toxicity at 3.5% (equivalent to 6.1 g/kg/day) as reduced number of litters, live pups per litter, and live pup weight. No such effects were seen at 1.75% (approximately 3.05 g/kg/day). The relevance of these very high dosages to human health is uncertain.
Pregnant rats receiving undiluted diethylene glycol by gavage over the period of organogenesis had toxic effects at 4.0 and 8.0 ml/kg/day as mortality, decreased body weight, decreased food consumption, increased water consumption, and increased liver and kidney weights. Fetotoxicity was seen only at these maternally toxic dosages. Decreased fetal body weight occurred at 8.0 ml/kg/day, and increased skeletal variants at 4.0 and 8.0 ml/kg/day. No embryotoxic or teratogenic effects were seen. Neither maternal toxicity nor fetotoxicity occurred at 1.0 ml/kg/day. In a study with mice also receiving undiluted diethylene glycol over the period of organogenesis, maternal toxicity occurred at 2.5 and 10.0 ml/kg/day, but not at 0.5 ml/kg/day. Definitive developmental toxicity was not seen in this species.

EMERGENCY AND FIRST AID PROCEDURES:

SWALLOWING:	If patient is fully conscious, give two glasses of water. Induce vomiting. This should be done only by medical or experienced first-aid personnel. Obtain medical attention.
SKIN:	Remove contaminated clothing. Wash skin with soap and water. Obtain medical attention if irritation persists. Wash clothing before reuse.
INHALATION:	No emergency care anticipated.
EYES:	Immediately flush eyes with water and continue washing for several minutes. Remove contact lenses, if worn. Obtain medical attention.
NOTES TO PHYSICIAN:	There is no specific antidote. Treatment of overexposure should be directed at the control of symptoms and the clinical condition of the patient.

VI. REACTIVITY DATA

STABILITY: Stable

CONDITIONS TO AVOID: Do not distill to dryness. Avoid excessive temperature or prolonged reflux, such as in batch distillations.
WARNING: Do not mix this product with nitrites or other nitrosating agents because a nitrosamine may be formed. Nitrosamines may cause cancer.

INCOMPATIBILITY (materials to avoid):
Strong alkalies.
High temperatures in the presence of strong bases.
Acids.
Strong oxidizing agents.

HAZARDOUS COMBUSTION OR DECOMPOSITION PRODUCTS:

Burning can produce the following products:
Carbon monoxide and/or carbon dioxide.
Oxides of Nitrogen.
Carbon monoxide is highly toxic if inhaled; carbon dioxide in sufficient concentrations can act as an asphyxiant.
Acute overexposure to the products of combustion may result in irritation of the respiratory tract.

HAZARDOUS POLYMERIZATION: Will Not Occur

CONDITIONS TO AVOID: None known.

VII. SPILL OR LEAK PROCEDURES

STEPS TO BE TAKEN IF MATERIAL IS RELEASED OR SPILLED:

Small spills can be flushed with large amounts of water; larger spills should be collected for disposal.
Wear suitable protective equipment.
Avoid contact with eyes.

WASTE DISPOSAL METHOD:

Incinerate in a furnace where permitted under Federal, State, and local regulations.
At very low concentrations in water, this product is biodegradable in a biological wastewater treatment plant.

VIII. SPECIAL PROTECTION INFORMATION

RESPIRATORY PROTECTION:

None expected to be needed.

VENTILATION: General (mechanical) room ventilation is expected to be satisfactory.

PROTECTIVE GLOVES: PVC-coated

EYE PROTECTION: Monogoggles

OTHER PROTECTIVE EQUIPMENT:

Eye Bath, Safety Shower

IX. SPECIAL PRECAUTIONS

PRECAUTIONS TO BE TAKEN IN HANDLING AND STORAGE:

WARNING!
CAUSES EYE IRRITATION.
MAY CAUSE ALLERGIC SKIN REACTION.
REPEATED BREATHING OF AEROSOL IN HIGH CONCENTRATIONS IS HARMFUL.

Avoid contact with eyes, skin and clothing.

Avoid repeated breathing of aerosol.
Keep container closed.
Use with adequate ventilation.
Wash thoroughly after handling.

Do not add nitrites or other nitrosating agents.
A nitrosamine, which may cause cancer, may be formed.

FOR INDUSTRY USE ONLY

OTHER PRECAUTIONS:

ADDITIONAL INFORMATION: There may be additional product safety information on this product, which may be obtained by calling your Union Carbide Corporation Sales or Customer Service Contact.

PROCESS HAZARD: Sudden release of hot organic chemical vapors or mists from process equipment operating at elevated temperature and pressure, or sudden ingress of air into hot equipment under a vacuum, may result in ignitions without the presence of obvious ignition sources. Published "autoignition" or "ignition" temperature values cannot be treated as safe operating temperatures in chemical processes without analysis of the actual process conditions.

Any use of this product in elevated-temperature processes should be thoroughly evaluated to establish and maintain safe operating conditions. Further information is available in a technical bulletin entitled "Ignition Hazards of Organic Chemical Vapors."

X. REGULATORY INFORMATION

STATUS ON SUBSTANCE LISTS:

The concentrations shown are maximum or ceiling levels (weight %) to be used for calculations for regulations. Trade Secrets are indicated by "TS".

FEDERAL EPA

Comprehensive Environmental Response Compensation, and Liability Act of 1980 (CERCLA) requires notification of the National Response Center of release of quantities of Hazardous Substances equal to or greater than the reportable quantities (RQs) in 40 CFR 302.4.

Components present in this product at a level which could require reporting under the statute are:

CHEMICAL	CAS NUMBER	UPPER BOUND CONCENTRATION %
Ethylene glycol monoethyl ether	110-80-5	0.01

In addition, this product contains other Glycol Ether(s) which, although included as a broad category on the CERCLA hazardous substance list, has not been assigned a reportable quantity.

Superfund Amendments and Reauthorization Act of 1986 (SARA) Title III requires emergency planning based on Threshold Planning Quantities (TPQs) and release reporting based on Reportable Quantities (RQs) in 40 CFR 355 (used for SARA 302, 304, 311 and 312).

Components present in this product at a level which could require reporting under the statute are:

*** NONE ***

Superfund Amendments and Reauthorization Act of 1986 (SARA) Title III requires submission of annual reports of release of toxic chemicals that appear in 40 CFR 372 (for SARA 313). This information must be included in all MSDSs that are copied and distributed for this material.

Components present in this product at a level which could require reporting under the statute are:

CHEMICAL	CAS NUMBER	UPPER BOUND CONCENTRATION %
Glycol Ethers	None	100

Toxic Substances Control Act (TSCA) STATUS:

All components of this product are on the TSCA Inventory or are exempt from TSCA Inventory requirements.

STATE RIGHT-TO-KNOW

CALIFORNIA Proposition 65

This product contains ETHYLENE GLYCOL MONOMETHYL ETHER and ETHYLENE GLYCOL MONOETHYL ETHER, known to the State of California to cause birth defects or other reproductive harm.
See Massachusetts listing for amounts.

MASSACHUSETTS Right-To-Know, Substance List (MSL) Hazardous Substances and Extraordinarily Hazardous Substances on the MSL must be identified when present in products.

Components present in this product at a level which could require reporting under the statute are:

HAZARDOUS SUBSTANCES (=> 1%)

CHEMICAL	CAS NUMBER	UPPER BOUND CONCENTRATION %
Diethylene Glycol Monomethyl Ether	111-77-3	4
Ethylene glycol monoethyl ether	110-80-5	0.01
Ethylene Glycol Monomethyl Ether	109-86-4	0.01

PENNSYLVANIA Right-to-Know, Hazardous Substance List Hazardous Substances and Special Hazardous Substances on the List must be identified when present in products.

Components present in this product at a level which could require reporting under the statute are:

HAZARDOUS SUBSTANCES (=> 1%)

CHEMICAL	CAS NUMBER	UPPER BOUND CONCENTRATION %
Glycol Ethers	None	100
Triethylene Glycol	112-27-6	10
Diethylene Glycol Monomethyl Ether	111-77-3	4
Diethylene Glycol	111-46-6	5

CALIFORNIA SCAQMD RULE 443.1 VOC'S:

***** NOT DETERMINED *****

PRODUCT NAME: EMKADIXOL 310 Brake Fluid

OTHER REGULATORY INFORMATION:

EPA Hazard Categories: Immediate Health, Delayed Health

NOTE ----

The opinions expressed herein are those of qualified experts within Union Carbide. We believe that the information contained herein is current as of the date of this Material Safety Data Sheet. Since the use of this information and the conditions of the use of the product are not under the control of Union Carbide, it is the user's obligation to determine conditions of safe use of the product.

REVISED SECTIONS:

SECTION III - INGREDIENTS
SECTION V - HEALTH HAZARD DATA
SECTION X - REGULATORY INFORMATION

PRODUCT: 31166
F NUMBER: C5008G

Appendix C

Electrochemical Equilibrium Reactions and E-pH Calculations for Copper-Water System

Rxn No.	REACTANTS								PRODUCTS							
	Cu+1	Cu+2	HCuO2-	CuO2-2	CuO	Cu2O	H+	H2O	e-	Cu	Cu+1	Cu+2	HCuO2-	CuO2-2	CuO	Cu2O	H+	H2O
	50.2	65.0	-257.0	-182.0	-119.7157	-146.4	0.0	-237.3	0.0	0.000	50.2	65.0	-257.0	-182.0	-119.7	-146.4	0.0	-237.3
1	0	0	1	0	0	0	3	0	0	0	0	1	0	0	0	0	0	2
2	0	0	0	1	0	0	4	0	0	0	0	1	0	0	0	0	0	2
3	0	0	0	1	0	0	1	0	0	0	0	1	0	0	0	0	0	0
4	0	1	0	0	0	0	0	1	0	0	1	0	0	0	0	0	0	2
5	0	0	1	0	0	0	3	0	1	0	0	1	0	0	0	0	0	2
6	0	0	0	1	0	0	4	0	1	0	0	1	0	0	0	0	0	2
7	0	0	0	0	0	1	2	0	2	0	0	0	0	0	0	0	0	1
8	0	0	0	0	1	0	2	0	2	1	0	0	0	0	0	0	0	1
9	0	0	0	0	2	0	2	0	2	0	0	0	0	0	0	1	0	1
10	0	0	0	0	0	1	2	0	0	0	2	0	0	0	0	0	0	1
11	0	0	0	0	1	0	2	0	0	0	0	1	0	0	0	0	0	1
12	0	0	0	1	0	0	1	0	0	0	0	0	0	0	1	0	0	1
13	0	0	0	0	0	0	2	0	0	0	0	0	0	0	1	0	0	1
14	1	0	0	0	0	0	0	0	1	1	0	0	0	0	0	0	0	0
15	0	1	0	0	0	0	0	0	1	0	0	0	0	0	0	0	0	0
16	0	0	1	0	0	0	3	0	2	1	0	0	0	0	0	0	0	0
17	0	0	0	0	0	0	4	0	2	1	0	0	0	0	0	0	0	2
18	0	2	0	0	0	0	4	0	2	1	0	0	0	0	0	0	0	2
19	0	0	2	0	0	0	4	0	2	0	0	0	0	0	0	0	2	0
20	0	0	0	2	0	0	6	0	2	0	0	0	0	0	0	1	0	3
21	0	0	0	0	1	0	2	0	1	0	1	0	0	0	0	0	0	1
Std. St.	1	1	1	1	1	1	1	1	1	1	1	1	1	1	1	1	1	1
Act.	1E-6	1E-6	1E-6	1E-6	1	1	1	1.0E+00	1	1	1E-6	1E-6	1E-6	1E-6	1	1	1	1

Input Data	
Ion Conc=	1.0E-06
Water Act.=	1.0E+00
R=	8.3144
F=	96480
T=	298.15
RT=	2478.93836
RT/F=	0.025692351
2.303*RT/F=	0.059216217

RESULTS

Rxn No.	ΔG	E(eq)°	Reactnt-Prod	Type of	E Intrcpt	Slope 1	Slope 2	E(eq)=fn(pH,pM) pM Intrcpt	Slope 1	Slope 2	pH(eq)=fn(E, pM) pH Intrcpt	Slope 1	Slope 2
	kJ/mol	Std. St.	Subst Type	Reaction	pH=0, pM=0	ΔE/ΔpH	ΔE/ΔpM *	E=0, pH=0	ΔpM/ΔE	ΔpM/ΔpH	E=0, pM=0	ΔpH/ΔE	ΔpH/ΔpM
1	-152.52	N/A	Diss-Diss	Non-Faradaic	--	--	--	26.7200	0	-3.0000	8.9067	0	-0.3333
2	-227.50	N/A	Diss-Diss	Non-Faradaic	--	--	--	39.8568	0	-4.0000	9.9642	0	-0.2500
3	-74.98	N/A	Diss-Diss	Non-Faradaic	--	--	--	13.1368	0	-1.0000	13.1368	0	-1.0000
4	-14.77	0.153	Diss-Diss	Faradaic	0.1531	0	0.0592	2.5875	16.9027	0	--	--	--
5	-167.29	1.734	Diss-Diss	Faradaic	1.7339	-0.1775	0.0592	29.3075	16.9027	-3.0000	9.7692	-5.6342	-0.3333
6	-242.27	2.511	Diss-Diss	Faradaic	2.5111	-0.2366	0.0592	42.4443	16.9027	-4.0000	10.6111	-4.2257	-0.2500
7	-90.88	0.471	Solid-Solid	Faradaic	0.4710	-0.0592	0	--	--	--	7.9608	-16.9027	0
8	-117.53	0.609	Solid-Solid	Faradaic	0.6091	-0.0592	0	--	--	--	10.2956	-16.9027	0
9	-144.19	0.747	Solid-Solid	Faradaic	0.7472	-0.0592	0	--	--	--	12.6305	-16.9027	0
10	9.54	N/A	Solid-Diss	Non-Faradaic	--	--	--	0.8354	0	1.0000	-0.8354	0	1.0000
11	-52.56	N/A	Solid-Diss	Non-Faradaic	--	--	--	-9.2076	0	2.0000	4.6038	0	0.5000
12	-99.96	N/A	Diss-Solid	Non-Faradaic	--	--	--	17.5123	0	-1.0000	17.5123	0	-1.0000
13	-174.94	N/A	Diss-Solid	Non-Faradaic	--	--	--	30.6491	0	-2.0000	15.3246	0	-0.5000
14	-50.21	0.520	Diss-Solid	Faradaic	0.5204	0	-0.0592	8.7961	-16.9027	0	--	--	--
15	-84.98	0.337	Diss-Solid	Faradaic	0.3367	0	-0.0296	11.3837	-33.8054	0	--	--	--
16	-217.49	1.127	Diss-Solid	Faradaic	1.1271	-0.0887	-0.0296	38.1036	-33.8054	-3.0000	12.7012	-11.2685	-0.3333
17	-292.48	1.516	Diss-Solid	Faradaic	1.5157	-0.1183	-0.0296	51.2404	-33.8054	-4.0000	12.8101	-8.4513	-0.2500
18	-39.06	0.203	Diss-Solid	Faradaic	0.2025	0.0592	-0.0592	3.4229	-16.9027	1.0000	-3.4229	16.9027	1.0000
19	-344.11	1.783	Diss-Solid	Faradaic	1.7833	-0.1183	-0.0592	30.1428	-16.9027	-2.0000	15.0714	-8.4513	-0.5000
20	-484.08	2.561	Diss-Solid	Faradaic	2.5605	-0.1775	-0.0592	43.2796	-16.9027	-3.0000	14.4265	-5.6342	-0.3333
21	-67.33	0.698	Solid-Diss	Faradaic	0.6978	-0.1183	0.0592	-11.7951	16.9027	2.0000	5.8976	-8.4513	0.5000

Rxn No.	REACTANTS									PRODUCTS								
	Cu+1	Cu+2	HCuO2-	CuO2-2	CuO	Cu2O	H+	H2O	e-	Cu	Cu+1	Cu+2	HCuO2-	CuO2-2	CuO	Cu2O	H+	H2O
	50.2	65.0	-257.0	-182.0	-119.7157	-146.4	0.0	-237.3	0.0	0.000	50.2	65.0	-257.0	-182.0	-119.7	-146.4	0.0	-237.3
1	0	0	1	0	0	0	3	0	0	0	0	1	0	0	0	0	0	2
2	0	0	0	1	0	0	4	0	0	0	0	1	0	0	0	0	0	2
3	0	0	0	1	0	0	1	0	0	0	0	0	1	0	0	0	0	0
4	0	1	0	0	0	0	0	0	1	0	1	0	0	0	0	0	0	0
5	0	0	1	0	0	0	3	0	1	0	1	0	0	0	0	0	0	2
6	0	0	0	1	0	0	4	0	1	0	1	0	0	0	0	0	0	2
7	0	0	0	0	0	1	2	0	2	2	0	0	0	0	0	0	0	1
8	0	0	0	0	1	0	2	0	2	1	0	0	0	0	0	0	0	1
9	0	0	0	0	2	0	2	0	2	0	0	0	0	0	0	1	0	1
10	0	0	0	0	0	1	2	0	0	0	2	0	0	0	0	0	0	1
11	0	0	0	0	1	0	2	0	0	0	0	1	0	0	0	0	0	1
12	0	0	1	0	0	0	1	0	0	0	0	0	0	0	0	1	0	1
13	0	0	0	1	0	0	2	0	0	0	0	0	0	0	0	1	0	1
14	1	0	0	0	0	0	0	0	1	1	0	0	0	0	0	0	0	0
15	0	1	0	0	0	0	0	0	2	1	0	0	0	0	0	0	0	0
16	0	0	1	0	0	0	3	0	2	1	0	0	0	0	0	0	0	2
17	0	0	0	1	0	0	4	0	2	1	0	0	0	0	0	0	0	2
18	0	2	0	0	0	0	0	1	2	0	0	0	0	0	0	1	2	0
19	0	0	2	0	0	0	4	0	2	0	0	0	0	0	0	1	0	3
20	0	0	0	2	0	0	6	0	2	0	0	0	0	0	0	1	0	3
21	0	0	0	0	1	0	2	0	1	0	1	0	0	0	0	0	0	1
Std. St.	1	1	1	1	1	1	1	1	1	1	1	1	1	1	1	1	1	1
Act.	1E-6	1E-6	1E-6	1E-6	1	1	1	1.0E-02	1	1	1E-6	1E-6	1E-6	1E-6	1	1	1	0.01

Input	Data
Ion Conc=	1.0E-06
Water Act.=	1.0E-02
R=	8.3144
F=	96480
T=	298.15
RT=	2478.93836
RT/F=	0.02569381
2.303*RT/F=	0.05916217

Rxn No.	RESULTS				E(eq)=fn(pH,pM)			pM(eq)=fn(E, pH)			pH(eq)=fn(E, pM)		
	ΔG	E(eq)°	Reactnt-Prod	Type of	E Intrcpt	Slope 1	Slope 2	pM Intrcpt	Slope 1	Slope 2	pH Intrcpt	Slope 1	Slope 2
	kJ/mol	Std. St.	Subst Type	Reaction	pH=0, pM=0	ΔE/ΔpH	ΔE/ΔpM *	E=0, pH=0	ΔpM/ΔE	ΔpM/ΔpH	E=0, pM=0	ΔpH/ΔE	ΔpH/ΔpM
1	-175.35	N/A	Diss-Diss	Non-Faradaic	∞	∞	∞	30.7200	0	-3.0000	10.2400	0	-0.3333
2	-250.33	N/A	Diss-Diss	Non-Faradaic	∞	∞	∞	43.8568	0	-4.0000	10.9642	0	-0.2500
3	-74.98	N/A	Diss-Diss	Non-Faradaic	∞	∞	∞	13.1368	0	-1.0000	13.1368	0	-1.0000
4	-14.77	0.153	Diss-Diss	Faradaic	0.1531	0	0.0592	2.5875	16.9027	0	∞	∞	∞
5	-190.12	1.971	Diss-Diss	Faradaic	1.9705	-0.1775	0.0592	33.3075	16.9027	-3.0000	11.1025	-5.6342	-0.3333
6	-265.10	2.748	Diss-Diss	Faradaic	2.7477	-0.2366	0.0592	46.4443	16.9027	-4.0000	11.6111	-4.2257	-0.2500
7	-102.30	0.530	Solid-Solid	Faradaic	0.5301	-0.0592	0	∞	∞	∞	8.9608	-16.9027	0
8	-128.95	0.668	Solid-Solid	Faradaic	0.6683	-0.0592	0	∞	∞	∞	11.2956	-16.9027	0
9	-155.60	0.806	Solid-Solid	Faradaic	0.8064	-0.0592	0	∞	∞	∞	13.6305	-16.9027	0
10	-1.88	N/A	Solid-Diss	Non-Faradaic	∞	∞	∞	-0.1646	0	1.0000	0.1646	0	1.0000
11	-63.97	N/A	Solid-Diss	Non-Faradaic	∞	∞	∞	-11.2076	0	2.0000	5.6038	0	0.5000
12	-111.38	N/A	Diss-Solid	Non-Faradaic	∞	∞	∞	19.5123	0	-1.0000	19.5123	0	-1.0000
13	-186.36	N/A	Diss-Solid	Non-Faradaic	∞	∞	∞	32.6491	0	-2.0000	16.3246	0	-0.5000
14	-50.21	0.520	Diss-Solid	Faradaic	0.5204	0	-0.0592	8.7961	-16.9027	0	∞	∞	∞
15	-64.98	0.337	Diss-Solid	Faradaic	0.3367	0	-0.0296	11.3837	-33.8054	0	∞	∞	∞
16	-240.33	1.245	Diss-Solid	Faradaic	1.2455	-0.0887	-0.0296	42.1036	-33.8054	-3.0000	14.0345	-11.2685	-0.3333
17	-315.31	1.634	Diss-Solid	Faradaic	1.6341	-0.1183	-0.0296	55.2404	-33.8054	-4.0000	13.8101	-8.4513	-0.2500
18	-27.66	0.143	Diss-Solid	Faradaic	0.1433	0.0592	-0.0592	2.4229	-16.9027	1.0000	-2.4229	16.9027	1.0000
19	-378.96	1.961	Diss-Solid	Faradaic	1.9608	-0.1183	-0.0592	33.1428	-16.9027	-2.0000	16.5714	-8.4513	-0.5000
20	-528.33	2.738	Diss-Solid	Faradaic	2.7380	-0.1775	-0.0592	46.2796	-16.9027	-3.0000	15.4265	-5.6342	-0.3333
21	-76.74	0.816	Solid-Diss	Faradaic	0.8162	-0.1183	0.0592	-13.7951	16.9027	2.0000	6.8976	-8.4513	0.5000

Rxn No.	REACTANTS									PRODUCTS								
	Cu+1	Cu+2	HCuO2-	CuO2-2	CuO	Cu2O	H+	H2O	e-	Cu	Cu+1	Cu+2	HCuO2-	CuO2-2	CuO	Cu2O	H+	H2O
	50.2	65.0	-257.0	-182.0	-119.7157	-146.4	0.0	-237.3	0.0	0.000	50.2	65.0	-257.0	-182.0	-119.7	-146.4	0.0	-237.3
1	0	0	1	0	0	0	3	0	0	0	0	1	0	0	0	0	0	2
2	0	0	0	1	0	0	4	0	0	0	0	1	0	0	0	0	0	2
3	0	0	0	1	0	0	1	0	0	0	0	0	1	0	0	0	0	0
4	0	1	0	0	0	0	0	0	1	0	1	0	0	0	0	0	0	0
5	0	0	1	0	0	0	3	0	1	0	1	0	0	0	0	0	0	2
6	0	0	0	1	0	0	4	0	1	0	1	0	0	0	0	0	0	2
7	0	0	0	0	0	1	2	0	2	2	0	0	0	0	0	0	0	1
8	0	0	0	0	1	0	2	0	2	1	0	0	0	0	0	0	0	1
9	0	0	0	0	2	0	2	0	2	0	0	0	0	0	0	1	0	1
10	0	0	0	0	0	1	2	0	0	0	2	0	0	0	0	0	0	1
11	0	0	0	0	1	0	2	0	0	0	0	1	0	0	0	0	0	1
12	0	0	1	0	0	0	1	0	0	0	0	0	0	0	0	1	0	1
13	0	0	0	1	0	0	2	0	0	0	0	0	0	0	0	1	0	1
14	1	0	0	0	0	0	0	0	1	1	0	0	0	0	0	0	0	0
15	0	1	0	0	0	0	0	0	2	1	0	0	0	0	0	0	0	0
16	0	0	1	0	0	0	3	0	2	1	0	0	0	0	0	0	0	2
17	0	0	0	1	0	0	4	0	2	1	0	0	0	0	0	0	0	2
18	0	2	0	0	0	0	0	1	2	0	0	0	0	0	0	1	2	0
19	0	0	2	0	0	0	4	0	2	0	0	0	0	0	0	1	0	3
20	0	0	0	2	0	0	6	0	2	0	0	0	0	0	0	1	0	3
21	0	0	0	0	1	0	2	0	1	0	1	0	0	0	0	0	0	1
Std. St.	1	1	1	1	1	1	1	1	1	1	1	1	1	1	1	1	1	1
Act.	1E-6	1E-6	1E-6	1E-6	1	1	1	1.0E-04	1	1	1E-6	1E-6	1E-6	1E-6	1	1	1	0.0001

Input	Data
Ion Concs=	1.0E-06
Water Act.=	1.0E-04
R=	8.3144
F=	96480
T=	298.15
RT=	2478.93836
RT/F=	0.02569381
2.303*RT/F=	0.05916217

Rxn No.	RESULTS				E(eq)=fn(pH,pM)			pM(eq)=fn(E, pH)			pH(eq)=fn(E, pM)		
	ΔG	E(eq)°	Reactnt-Prod	Type of	E Intrcpt	Slope 1	Slope 2	pM Intrcpt	Slope 1	Slope 2	pH Intrcpt	Slope 1	Slope 2
	kJ/mol	Std. St.	Subst Type	Reaction	pH=0, pM=0	ΔE/ΔpH	ΔE/ΔpM *	E=0, pH=0	ΔpM/ΔE	ΔpM/ΔpH	E=0, pM=0	ΔpH/ΔE	ΔpH/ΔpM
1	-198.18	N/A	Diss-Diss	Non-Faradaic	∞	∞	∞	34.7200	0	-3.0000	11.5733	0	-0.3333
2	-273.16	N/A	Diss-Diss	Non-Faradaic	∞	∞	∞	47.8568	0	-4.0000	11.9642	0	-0.2500
3	-74.98	N/A	Diss-Diss	Non-Faradaic	∞	∞	∞	13.1368	0	-1.0000	13.1368	0	-1.0000
4	-14.77	0.153	Diss-Diss	Faradaic	0.1531	0	0.0592	2.5875	16.9027	0	∞	∞	∞
5	-212.95	2.207	Diss-Diss	Faradaic	2.2072	-0.1775	0.0592	37.3075	16.9027	-3.0000	12.4358	-5.6342	-0.3333
6	-287.93	2.984	Diss-Diss	Faradaic	2.9844	-0.2366	0.0592	50.4443	16.9027	-4.0000	12.6111	-4.2257	-0.2500
7	-113.71	0.589	Solid-Solid	Faradaic	0.5893	-0.0592	0	∞	∞	∞	9.9608	-16.9027	0
8	-140.37	0.727	Solid-Solid	Faradaic	0.7274	-0.0592	0	∞	∞	∞	12.2956	-16.9027	0
9	-167.02	0.866	Solid-Solid	Faradaic	0.8656	-0.0592	0	∞	∞	∞	14.6305	-16.9027	0
10	-13.30	N/A	Solid-Diss	Non-Faradaic	∞	∞	∞	-1.1646	0	1.0000	1.1646	0	1.0000
11	-75.39	N/A	Solid-Diss	Non-Faradaic	∞	∞	∞	-13.2076	0	2.0000	6.6038	0	0.5000
12	-122.79	N/A	Diss-Solid	Non-Faradaic	∞	∞	∞	21.5123	0	-1.0000	21.5123	0	-1.0000
13	-197.78	N/A	Diss-Solid	Non-Faradaic	∞	∞	∞	34.6491	0	-2.0000	17.3246	0	-0.5000
14	-50.21	0.520	Diss-Solid	Faradaic	0.5204	0	-0.0592	8.7961	-16.9027	0	∞	∞	∞
15	-64.98	0.337	Diss-Solid	Faradaic	0.3367	0	-0.0296	11.3837	-33.8054	0	∞	∞	∞
16	-263.16	1.364	Diss-Solid	Faradaic	1.3638	-0.0887	-0.0296	46.1036	-33.8054	-3.0000	15.3679	-11.2685	-0.3333
17	-338.14	1.752	Diss-Solid	Faradaic	1.7524	-0.1183	-0.0296	59.2404	-33.8054	-4.0000	14.8101	-8.4513	-0.2500
18	-16.24	0.084	Diss-Solid	Faradaic	0.0842	0.0592	-0.0592	1.4229	-16.9027	1.0000	-1.4229	16.9027	1.0000
19	-412.60	2.136	Diss-Solid	Faradaic	2.1383	-0.1183	-0.0592	36.1428	-16.9027	-2.0000	18.0714	-8.4513	-0.5000
20	-562.57	2.915	Diss-Solid	Faradaic	2.9155	-0.1775	-0.0592	49.2796	-16.9027	-3.0000	16.4265	-5.6342	-0.3333
21	-90.16	0.934	Solid-Diss	Faradaic	0.9345	-0.1183	0.0592	-15.7951	16.9027	2.0000	7.8976	-8.4513	0.5000

Rxn No.	REACTANTS									PRODUCTS								
	Cu+1	Cu+2	HCuO2-	CuO2-2	CuO	Cu2O	H+	H2O	e-	Cu	Cu+1	Cu+2	HCuO2-	CuO2-2	CuO	Cu2O	H+	H2O
	50.2	65.0	-257.0	-182.0	-119.7157	-146.4	0.0	-237.3	0.0	0.000	50.2	65.0	-257.0	-182.0	-119.7	-148.4	0.0	-237.3
1	0	0	1	0	0	0	3	0	0	0	0	1	0	0	0	0	0	2
2	0	0	0	1	0	0	4	0	0	0	0	1	0	0	0	0	0	2
3	0	0	0	1	0	0	1	0	0	0	0	0	1	0	0	0	0	0
4	0	1	0	0	0	0	0	0	1	0	1	0	0	0	0	0	0	0
5	0	0	1	0	0	0	3	0	1	0	1	0	0	0	0	0	0	2
6	0	0	0	1	0	0	4	0	1	0	1	0	0	0	0	0	0	2
7	0	0	0	0	0	1	2	0	2	2	0	0	0	0	0	0	0	1
8	0	0	0	0	1	0	2	0	2	1	0	0	0	0	0	0	0	1
9	0	0	0	0	2	0	2	0	2	0	0	0	0	0	0	1	0	1
10	0	0	0	0	0	1	2	0	0	0	2	0	0	0	0	0	0	1
11	0	0	0	0	1	0	2	0	0	0	0	1	0	0	0	0	0	1
12	0	0	1	0	0	0	1	0	0	0	0	0	0	0	0	1	0	1
13	0	0	0	1	0	0	2	0	0	0	0	0	0	0	0	1	0	1
14	1	0	0	0	0	0	0	0	1	1	0	0	0	0	0	0	0	0
15	0	1	0	0	0	0	0	0	2	1	0	0	0	0	0	0	0	0
16	0	0	1	0	0	0	3	0	2	1	0	0	0	0	0	0	0	2
17	0	0	0	1	0	0	4	0	2	1	0	0	0	0	0	0	0	2
18	0	2	0	0	0	0	0	1	2	0	0	0	0	0	0	1	2	0
19	0	0	2	0	0	0	4	0	2	0	0	0	0	0	0	1	0	3
20	0	0	0	2	0	0	6	0	2	0	0	0	0	0	0	1	0	3
21	0	0	0	0	1	0	2	0	1	0	1	0	0	0	0	0	0	1
Std. St.	1	1	1	1	1	1	1	1	1	1	1	1	1	1	1	1	1	1
Act.	1E-6	1E-6	1E-6	1E-6	1	1	1	1.0E-06	1	1	1E-6	1E-6	1E-6	1E-6	1	1	1	0.000001

Input	Data
Ion Concs=	1.0E-06
Water Act.=	1.0E-06
R=	8.3144
F=	96480
T=	298.15
RT=	2478.93836
RT/F=	0.02569381
2.303*RT/F=	0.05916217

Rxn No.	RESULTS				E(eq)=fn(pH,pM)			pM(eq)=fn(E, pH)			pH(eq)=fn(E, pM)		
	ΔG	E(eq)°	Reactnt-Prod	Type of	E Intrcpt	Slope 1	Slope 2	pM Intrcpt	Slope 1	Slope 2	pH Intrcpt	Slope 1	Slope 2
	kJ/mol	Std. St.	Subst Type	Reaction	pH=0, pM=0	ΔE/ΔpH	ΔE/ΔpM *	E=0, pH=0	ΔpM/ΔE	ΔpM/ΔpH	E=0, pM=0	ΔpH/ΔE	ΔpH/ΔpM
1	-221.01	N/A	Diss-Diss	Non-Faradaic	∞	∞	∞	38.7200	0	-3.0000	12.9067	0	-0.3333
2	-296.00	N/A	Diss-Diss	Non-Faradaic	∞	∞	∞	51.8568	0	-4.0000	12.9642	0	-0.2500
3	-74.98	N/A	Diss-Diss	Non-Faradaic	∞	∞	∞	13.1368	0	-1.0000	13.1368	0	-1.0000
4	-14.77	0.153	Diss-Diss	Faradaic	0.1531	0	0.0592	2.5875	16.9027	0	∞	∞	∞
5	-235.78	2.444	Diss-Diss	Faradaic	2.4438	-0.1775	0.0592	41.3075	16.9027	-3.0000	13.7692	-5.6342	-0.3333
6	-310.77	3.221	Diss-Diss	Faradaic	3.2210	-0.2366	0.0592	54.4443	16.9027	-4.0000	13.6111	-4.2257	-0.2500
7	-125.13	0.648	Solid-Solid	Faradaic	0.6485	-0.0592	0	∞	∞	∞	10.9608	-16.9027	0
8	-151.78	0.787	Solid-Solid	Faradaic	0.7866	-0.0592	0	∞	∞	∞	13.2956	-16.9027	0
9	-178.44	0.925	Solid-Solid	Faradaic	0.9247	-0.0592	0	∞	∞	∞	15.6305	-16.9027	0
10	-24.71	N/A	Solid-Diss	Non-Faradaic	∞	∞	∞	-2.1646	0	1.0000	2.1646	0	1.0000
11	-86.80	N/A	Solid-Diss	Non-Faradaic	∞	∞	∞	-15.2076	0	2.0000	7.6038	0	0.5000
12	-134.21	N/A	Diss-Solid	Non-Faradaic	∞	∞	∞	23.5123	0	-1.0000	23.5123	0	-1.0000
13	-209.19	N/A	Diss-Solid	Non-Faradaic	∞	∞	∞	36.6491	0	-2.0000	18.3246	0	-0.5000
14	-50.21	0.520	Diss-Solid	Faradaic	0.5204	0	-0.0592	8.7961	-16.9027	0	∞	∞	∞
15	-64.98	0.337	Diss-Solid	Faradaic	0.3367	0	-0.0296	11.3837	-33.8054	0	∞	∞	∞
16	-285.99	1.482	Diss-Solid	Faradaic	1.4821	-0.0887	-0.0296	50.1036	-33.8054	-3.0000	16.7012	-11.2685	-0.3333
17	-360.97	1.871	Diss-Solid	Faradaic	1.8707	-0.1183	-0.0296	63.2404	-33.8054	-4.0000	15.8101	-8.4513	-0.2500
18	-4.83	0.025	Diss-Solid	Faradaic	0.0250	0.0592	-0.0592	0.4229	-16.9027	1.0000	-0.4229	16.9027	1.0000
19	-446.85	2.316	Diss-Solid	Faradaic	2.3158	-0.1183	-0.0592	39.1428	-16.9027	-2.0000	19.5714	-8.4513	-0.5000
20	-596.82	3.093	Diss-Solid	Faradaic	3.0930	-0.1775	-0.0592	52.2796	-16.9027	-3.0000	17.4265	-5.6342	-0.3333
21	-101.57	1.059	Solid-Diss	Faradaic	1.0528	-0.1183	0.0592	-17.7951	16.9027	2.0000	8.8976	-8.4513	0.5000